MCB
Journals.ASM.org

The TAF9 C-Terminal Conserved Region Domain Is Required for SAGA and TFIID Promoter Occupancy To Promote Transcriptional Activation

Malika Saint,[a] Sonal Sawhney,[a] Ishani Sinha,[a] Rana Pratap Singh,[a] Rashmi Dahiya,[a] Anushikha Thakur,[a] Rahul Siddharthan,[b] Krishnamurthy Natarajan[a]

Laboratory of Eukaryotic Gene Regulation, School of Life Sciences, Jawaharlal Nehru University, New Delhi, India[a]; Institute of Mathematical Sciences, Taramani, Chennai, Tamil Nadu, India[b]

A common function of the TFIID and SAGA complexes, which are recruited by transcriptional activators, is to deliver TBP to promoters to stimulate transcription. Neither the relative contributions of the five shared TBP-associated factor (TAF) subunits in TFIID and SAGA nor the requirement for different domains in shared TAFs for transcriptional activation is well understood. In this study, we uncovered the essential requirement for the highly conserved C-terminal region (CRD) of Taf9, a shared TAF, for transcriptional activation in yeast. Transcriptome profiling performed under Gcn4-activating conditions showed that the Taf9 CRD is required for induced expression of ~9% of the yeast genome. The CRD was not essential for the Taf9-Taf6 interaction, TFIID or SAGA integrity, or Gcn4 interaction with SAGA in cell extracts. Microarray profiling of a SAGA mutant (*spt20*Δ) yielded a common set of genes induced by Spt20 and the Taf9 CRD. Chromatin immunoprecipitation (ChIP) assays showed that, although the Taf9 CRD mutation did not impair Gcn4 occupancy, the occupancies of TFIID, SAGA, and the preinitiation complex were severely impaired at several promoters. These results suggest a crucial role for the Taf9 CRD in genome-wide transcription and highlight the importance of conserved domains, other than histone fold domains, as a common determinant for TFIID and SAGA functions.

Biological systems contain several multisubunit transcription complexes bearing one or more shared protein subunits. Such complexes regulate transcription at various levels and are well studied in the yeast *Saccharomyces cerevisiae* (1–4). Transcriptional activation is a multistep process that regulates gene expression under various conditions. A variety of transcription factors and regulatory complexes are recruited in a specific manner to gene promoters in response to activating stimuli (2, 5).

Gcn4, a master transcriptional activator during amino acid starvation response and other stress (6), binds to the upstream activation sequence (UAS) regions of target promoters and recruits a wide array of coactivators (7–11), including the SAGA histone acetyltransferase complex and SWI/SNF chromatin-remodeling complex to remodel chromatin. The permissive chromatin then allows stable assembly of the preinitiation complex (PIC), composed of the general transcription factors (GTFs) TFIIA, -B, -D, -E, -F, and -H and RNA polymerase II (RNAP II), in the core promoter region (2, 3, 5, 12). TBP delivery is a key rate-limiting step in the PIC assembly process (13, 14). Two pathways have been identified for TBP delivery: TATA-containing promoters assemble TBP primarily through the SAGA pathway, whereas the TATA-like (noncanonical TATA) promoters assemble TBP through the TFIID pathway (15–19).

Genetic and genomic experiments suggest that SAGA and TFIID have redundant roles in transcription (15, 20). Whereas inactivation of the TFIID subunit Taf1 (*taf1*^{ts2}) or the SAGA subunit Spt3 (*spt3*Δ) or Gcn5 (*gcn5*Δ) individually reduced transcription of a limited number of genes, transcription was completely shut down in the *taf1 spt3* or *taf1 gcn5* double mutants, indicating redundancy of TFIID and SAGA complexes in transcription. However, it is unclear what facets of TFIID and SAGA function are impaired in the double mutant (15, 20).

Since the discovery that 5 of the 14 TBP-associated factors (TAFs) are shared in the TFIID and SAGA complexes (21–23), little information has been available about their relative roles in the two complexes. Of central importance is whether the shared TAF subunits have similar roles in the TFIID and SAGA complexes or if they perform complex-specific roles. The shared protein subunits also contain one or more evolutionarily conserved domains (24), and it remains to be seen if such domains contribute differently to TFIID and SAGA complex functions.

Taf9 is an evolutionarily conserved subunit of the SAGA and TFIID complexes. The evolutionary conservation of yeast Taf9 spans the amino-terminal histone H3-like histone fold domain (HFD) and the carboxyl-terminal conserved region domain (CRD), but in higher eukaryotes, an additional carboxyl-terminal extension is present (25). The requirement for Taf9 for transcription was previously studied using conditional alleles or depletion strategies in yeast and higher eukaryotes (26–29). However, the mutant yeast *taf9* alleles employed had multiple mutations and/or led to a total depletion of the Taf9 mutant protein levels, thereby making it difficult to assess the direct contributions of Taf9.

Received 14 August 2013 **Returned for modification** 3 September 2013
Accepted 20 January 2014
Published ahead of print 18 February 2014
Address correspondence to Krishnamurthy Natarajan, nat0200@gmail.com.
M.S. and S.S. made equal contributions to the article.
Supplemental material for this article may be found at http://dx.doi.org/10.1128/MCB.01060-13.

doi:10.1128/MCB.01060-13

The Taf9 HFD appears sufficient for dimerization with Taf6, as was evident from the Taf9-Taf6 crystal structure (30), and due to copurification of a C-terminally truncated yeast Taf9 mutant with TFIID (31). The Taf9 C-terminal region interacts with the downstream promoter element (DPE), located around +30 with respect to the transcription start site in *Drosophila* and humans (25, 32). Studies in mammalian cells showed an intriguing requirement for the C-terminal region for Taf9 interaction with both the zinc finger domain of the hematopoiesis-specific transcription factor EKLF and the DPE of the β-globin gene, an EKLF target (33). The DPE is notably absent in yeast (2, 32). The Taf9 CRD has been shown to be important for interaction of TFIID with the yeast cell cycle regulator Swi6 (31, 34). However, none of the previous studies examined if the Taf9 CRD was required for Taf9 association with SAGA or for SAGA function. Moreover, a requirement for the CRD for genome-wide transcription has also not been probed before.

In this study, we provide several lines of evidence to demonstrate that the evolutionarily conserved Taf9 CRD is a critical domain required for transcriptional activation. The Taf9 CRD is required for induced expression of ~9% of yeast genes under amino acid starvation conditions. Chromatin immunoprecipitation (ChIP) assays showed that promoter occupancy of SAGA, TFIID, and PIC require the Taf9 CRD under Gcn4-activating conditions for several but not all promoters examined. Thus, we have uncovered a critical role for the Taf9 CRD in SAGA- and TFIID-mediated transcriptional activation and PIC assembly at both Gcn4-dependent and -independent promoters *in vivo*.

MATERIALS AND METHODS

Strains, plasmids, and oligonucleotides. The strains, plasmids, and oligonucleotides used in this study are listed in Tables S1, S2, and S3 in the supplemental material, respectively.

Media and growth conditions. *S. cerevisiae* strains were cultured in synthetic complete (SC) medium containing 1.5 g/liter Bacto-Yeast Nitrogen Base with ammonium sulfate with added amino acid supplements or in yeast extract-peptone-dextrose (YPD) medium. Yeast cells were cultured in SC-Leu-Ile-Val medium with sulfometuron methyl (SM) to impose amino acid starvation conditions, using different concentrations of SM, as indicated.

Error-prone PCR mutagenesis and gap repair cloning of Taf9 mutants. Random mutations were introduced into the *TAF9* gene by error-prone PCR using *Taq* DNA polymerase (35). Each 100-μl reaction mixture contained 1.75 mM $MgCl_2$, 0.25 mM $MnCl_2$, 0.4 mM (each) dCTP, dTTP, and dGTP, and 0.1 mM dATP, as well as 0.3 μM (each) forward and reverse primers, ON294 and ON299, respectively; 2.5 U *Taq* DNA polymerase; and 0.4 ng of plasmid Sp1 as template DNA. The PCR products were digested with EcoRV. The vector Sp1 was cut with BseJI and BamHI, and the gapped vector and insert were mixed in a molar ratio of 1:3 and transformed (36) into yeast strain RPY1. To identify recessive *taf9* alleles, the *URA3*-marked *TAF9* plasmid Ip1 was shuffled out from yeast strains on 5-fluoroorotic acid (5-FOA)-containing medium and tested for SM sensitivity. A total of 5,250 transformants were screened, resulting in 63 potential candidates. The mutant *taf9* plasmids were rescued, retransformed into strain RPY1, and retested. A total of 35 candidates showed a reproducible SM-sensitive growth phenotype.

RNA isolation and real-time PCR analysis. Total RNA was isolated by the hot-phenol method (37) according to details provided under Gene Expression Omnibus (GEO) accession number GSE44544. About 500 ng of total RNA was treated with DNase I, Amplification grade (Invitrogen), and used for cDNA synthesis using the ABI High Capacity cDNA reverse transcription kit. Quantitative PCR (qPCR) was carried out using SYBR green chemistry in an ABI 7500 or ABI 7500 Fast real-time (RT) PCR system according to the manufacturer's cycling conditions. All real-time PCR primers were verified to have an amplification efficiency of at least 1.9 ± 0.06. The Pol III-transcribed *scR1* RNA was used as the endogenous control. The concordant data (the threshold cycle [C_T] values of outliers were removed when the replicate C_T difference was >1.0) were averaged from a minimum of two biological-replicate RNA preparations. The relative gene expression was calculated using the $2^{-\Delta\Delta CT}$ method (38, 39).

Expression profiling and analysis. Total RNA was isolated by the hot-phenol method from the RPY72 (wild-type [WT]), YSS26 (*taf9-tCRD2*), and *spt20*Δ (number 7390; Open Biosystems) strains, treated or not with SM, and the RNA was purified using the RNeasy kit (Qiagen). Four independent RNA preparations were made from each of the untreated or SM-treated WT (WT ± SM) and *taf9* (*taf9* ± SM) strains and two independent preparations from the *spt20*Δ strain treated with SM. Four microarray hybridizations, including two dye swaps, were conducted for the WT ± SM, *taf9* ± SM, and *taf9-tCRD2* plus SM/WT plus SM and two dye-swap hybridizations for the *spt20*Δ plus SM/WT plus SM comparison were performed. RNA samples were processed and hybridized using the two-color protocol to custom 8×15k yeast gene expression arrays (Agilent). Raw data were extracted using Agilent feature extraction software v. 10.7.3.1, and the two-color data were normalized using the LOWESS option in GeneSpring GX 12.5 software.

Statistically significant differential expression in the WT ± SM, *taf9* ± SM, and *taf9-tCRD2* plus SM/WT plus SM comparisons was determined using the significance analysis of microarrays (SAM) tool (40) at a false discovery rate (FDR) of ~5% in all experiments. Additionally, Bayesian analysis was independently carried out using the BAGEL tool (41) with default settings. Genes that showed nonoverlapping confidence intervals were selected as being significantly differentially expressed in each experiment.

Genes found to be significantly differentially expressed by both SAM and BAGEL were further filtered through a PERL script for genes that showed consistent (at least 3 of the 4 arrays in each experiment) differential expression of at least 1.5-fold (a $\log_2$ ratio of ≥0.585 for upregulated and ≤−0.585 for downregulated genes) in WT ± SM data were selected for further analysis. BAGEL was also used to identify genes that showed no expression change (a $\log_2$ ratio ≤0.585 and ≥−0.585) in the *taf9* ± SM arrays. The WT ± SM and the *spt20*Δ plus SM/WT plus SM data were analyzed using BAGEL, and genes showing statistically significant differential expression were determined as described above. For the *spt20*Δ plus SM/WT plus SM arrays, genes that showed differential expression of at least 1.5-fold in both arrays were selected. Only those open reading frames (ORFs) identified as being in verified and uncharacterized categories, based on the chromosomal feature file (downloaded in January 2013) from the *Saccharomyces* Genome Database, were used for further analysis.

The Taf9 CRD-dependent genes were identified from three comparisons: (i) Genes with no change in expression in the *taf9* ± SM data relative to their values in the WT ± SM data, (ii) genes with either $\log_2$ ratios of ≤−0.585 or ≥0.585 in the *taf9-tCRD2* plus SM/WT plus SM data and either up- or downregulated (at least 1.5-fold) in the WT ± SM data, and (iii) genes whose expression values in the *taf9* ± SM data differed by 1.5-fold from those in the WT ± SM data. A total of 963 genes were derived from this analysis, from which genes whose $\log_2$ ratios were greater in the *taf9* ± SM and *taf9* plus SM/WT plus SM data by a factor of 1.5-fold relative to their values in the WT ± SM data were removed to yield 463 genes that required the Taf9 CRD for their induction. A similar analysis was done for the downregulated set to yield 400 genes that required the Taf9 CRD for their repression.

Clustering analysis was performed using hierarchical clustering of the 963 Taf9 CRD-dependent genes using GeneSpring GX 12.5 software (Agilent). Dubious ORFs were removed from the 538 Gcn4-induced genes identified previously (42), and the resulting 515 Gcn4-induced genes were used for analysis. Details of the meta-analysis of the Gcn4 ChIP-on-chip data and the statistical analysis of the significance of the overlap in the Venn diagram are provided in the supplemental material.

Coimmunoprecipitation and GST-Gcn4 pulldown assays. Coimmunoprecipitation was carried out from whole-cell extracts prepared as described previously (43), using an anti-Myc mouse monoclonal antibody (Roche) essentially as described previously (9, 23), except that the antibody was cross-linked to protein G-Sepharose 4B beads using dimethyl pimelimidate (Fluka). The glutathione *S*-transferase (GST)–Gcn4 pulldown assays were performed essentially as described previously (9, 23). The pulldown material was run on 6 to 12% SDS-PAGE gels, Western blotted, and probed with the indicated antibodies using ECL Plus reagent (GE Healthcare).

Chromatin immunoprecipitation. Chromatin extracts were prepared essentially as described previously (44, 45). The cells were cultured with or without SM treatment, as described above (GEO accession number GSE44544). Yeast cell cultures (optical density at 600 nm [OD_{600}], 100 to 140) were cross-linked with 20 ml of formaldehyde solution (50 mM HEPES-KOH, pH 7.5, 1 mM EDTA, 140 mM NaCl, and 11% [vol/vol] formaldehyde) for 20 min with intermittent shaking and then quenched with 30 ml 2.5 M glycine for 5 min at ambient temperature. Cells were collected by centrifugation and washed sequentially with 200 ml and 100 ml cold Tris-buffered saline. The cells were lysed in 400 μl FA lysis buffer (50 mM HEPES-KOH [pH 7.5], 1 mM EDTA, 140 mM NaCl, 1% Triton X-100, 0.1% sodium deoxycholate, and protease inhibitors) using acid-washed and dried glass beads for 45 min in a Vortex Genie (Scientific Industries). The lysate was sonicated in ice using the Branson 250D sonicator set to 14 to 16% amplitude, with a 12-s pulse each cycle for a total of 20 to 25 cycles. The chromatin extracts were stored at −80°C, and prior to use, the chromatin extract was cleared by centrifugation in 1.5-ml tubes at 13,000 rpm for 30 min at 4°C. DNA was extracted, and the chromatin size was ensured each time to be in the average range of ~300 to 500 bp. For immunoprecipitation (IP) reactions, protein G-Sepharose beads (GE Healthcare) were washed with 1× phosphate-buffered saline (PBS), and 12.5 μg anti-Myc antibody, or 2 to 3 μg of other antibodies, per IP was bound to 12.5-μl beads for 2 h at 4°C. Chromatin extracts equivalent to cells at an OD_{600} of ~20 were added to the antibody-coupled beads in FA lysis buffer, and IPs were conducted for 2 h at 4°C. The immune complexes were washed for 3 min each at room temperature and eluted in 125 μl as described previously (46). The eluted DNA was de-cross-linked overnight at 65°C, treated with RNase A (100 μg/ml) for 2 h at 37°C, and then treated with proteinase K (0.4 μg/ml) for 30 min at 42°C, and samples were phenol-chloroform extracted and DNA precipitated with 3 volumes of ethanol in the presence of LiCl and glycogen as a carrier. The DNA was resuspended in 50 μl 0.1× Tris-EDTA (TE) and used for PCR analysis. The input total DNA was diluted 10,000-fold, and the IP DNA samples were diluted between ~2- and 10-fold and used for quantitative real-time PCR using SYBR green chemistry. All primers used for qPCR had an amplification efficiency of at least 1.9 ± 0.06. The fold enrichment was determined using the $2^{-\Delta\Delta CT}$ relative-quantitation method (38, 39). The C_T values were used to calculate the enrichment of IP DNA relative to the input DNA ($\Delta C_T = C_T$ input $- C_T$ IP) for a specific target, as well as the nonspecific control *POL1* coding sequence or the TEL06R-XC (for H3 acetyl-K9/14 [K9/14Ac] IPs). The ΔC_T value of the specific target was subtracted from that of *POL1* to calculate the enrichment of specific DNA with reference to the control nonspecific DNA ($\Delta\Delta C_T = \Delta C_T$ target $- \Delta C_T$ control), and $2-^{\Delta\Delta CT}$ was calculated (38, 39). The *GPM1* UAS locus was analyzed using the absolute relative quantitation method (38, 39).

Antibodies. The following antibodies were used for ChIP or Western blot analysis: mouse monoclonal anti-c-Myc clone 9E10 (catalog no. 11667203001; Roche), mouse monoclonal Rpb1 8WG16 (catalog no. ab817; Abcam), rabbit polyclonal anti-acetyl-histone H3 (catalog no. 06-599; Upstate-Millipore), rabbit polyclonal histone H3 antibody (catalog no. ab46765; Abcam), rabbit polyclonal Rpb1 phospho-Ser2 (catalog no. ab5095; Abcam), mouse polyclonal antihemagglutinin (anti-HA) clone 12CA5 (47), rabbit polyclonal anti-Taf12 (48), and rabbit polyclonal anti-Gcn4 (8). Other antibodies used were anti-Gcn5 (49), Snf6 (a kind gift from Alan Hinnebusch), anti-Taf1 (50), anti-Tra1 (51), rabbit polyclonal TBP (52), and anti-Taf5 and anti-Taf6 antibodies (a kind gift from Tony Weil [53]).

Microarray data accession number. The microarray data have been deposited at NCBI Gene Expression Omnibus under accession number GSE44544.

RESULTS

A genetic screen identified the requirement for TAF9 CRD for Gcn4-dependent transcriptional activation. In a genetic screen to identify regions of Taf9 required for transcriptional activation by Gcn4, we screened for mutants impaired for growth in SM, an inhibitor of isoleucine and valine biosynthesis, which induces Gcn4 expression (6, 54). A total of 35 candidates that conferred a reproducible SM-sensitive phenotype were obtained, 9 of which showed a very severe phenotype. The *TAF9* ORF from each of the nine mutants was subcloned to a fresh vector backbone to eliminate any unrelated mutations outside the coding region, and their SM-sensitive phenotype was reconfirmed by spot assay (Fig. 1A). All of the mutants also exhibited a temperature-sensitive phenotype (Fig. 1A). Sequencing of the *TAF9* coding region revealed that each mutant had one or more mutations, but remarkably, all the mutants contained a premature stop codon (Fig. 1A), indicating that the Taf9 CRD was truncated to various extents.

To further understand the CRD function, systematic deletion constructs of *TAF9* bearing a premature stop codon at amino acid residues 106, 121, and 132 were made and named Taf9-tCRD1, -tCRD3, and -tCRD2, respectively (Fig. 1B). These *taf9-CRD* mutants were designed by making the C-terminal region (amino acids 102 to 157) into three segments as follows: the *tCRD1* truncation removed the entire C-terminal region up to the HF domain, the *tCRD2* truncation retained amino acids up to the predicted fourth α-helix (shown in the schematic below yTAF9 in Fig. 1B), and *tCRD3* retained amino acids including a partial region of the predicted fourth α-helix. Whereas the *taf9-tCRD1* and *-tCRD3* mutants caused lethality, the *taf9-tCRD2* mutant was viable (Fig. 1C). Western blot analysis showed that all the mutant proteins are stably expressed (Fig. 1D, lanes 5 to 8) at or above the level of the WT Taf9 in the same strains (Fig. 1D, lanes 6 to 8). Thus, the lethality of the *taf9-tCRD1* and *-tCRD3* mutants was not a consequence of defective expression. The *taf9-tCRD2*-bearing strain showed an extreme SM-sensitive phenotype and a lethal phenotype at 37°C (Fig. 1E). In the viable *taf9-tCRD2* strain, the level of the mutant Taf9-tCRD2 protein was comparable to that of WT Taf9 (Fig. 1D, compare lane 5 with lane 3). To be sure, we further introduced the *taf9-tCRD2* allele on a high-copy-number plasmid, confirmed the overexpression, and found that the *taf9-tCRD2* mutant phenotype was not altered (see Fig. S1 in the supplemental material).

In a previous study, it was reported that Taf9 has genetic interactions with components of the transcription elongation machinery (55). Moreover, the ySAGA complex has also been implicated in the process of transcriptional elongation (45, 56, 57). To distinguish if the mutant phenotype is due to an impairment of transcription initiation or elongation processes, we examined the growth of the WT and the *taf9* mutant in media containing the elongation inhibitor mycophenolic acid (MPA) or 6-azauracil (6-AU) (58). The *taf9-tCRD2* mutant did not show a growth defect in MPA or 6-AU (Fig. 1F), indicating that the Taf9 CRD is not required for global transcription elongation. This conclusion is fur-

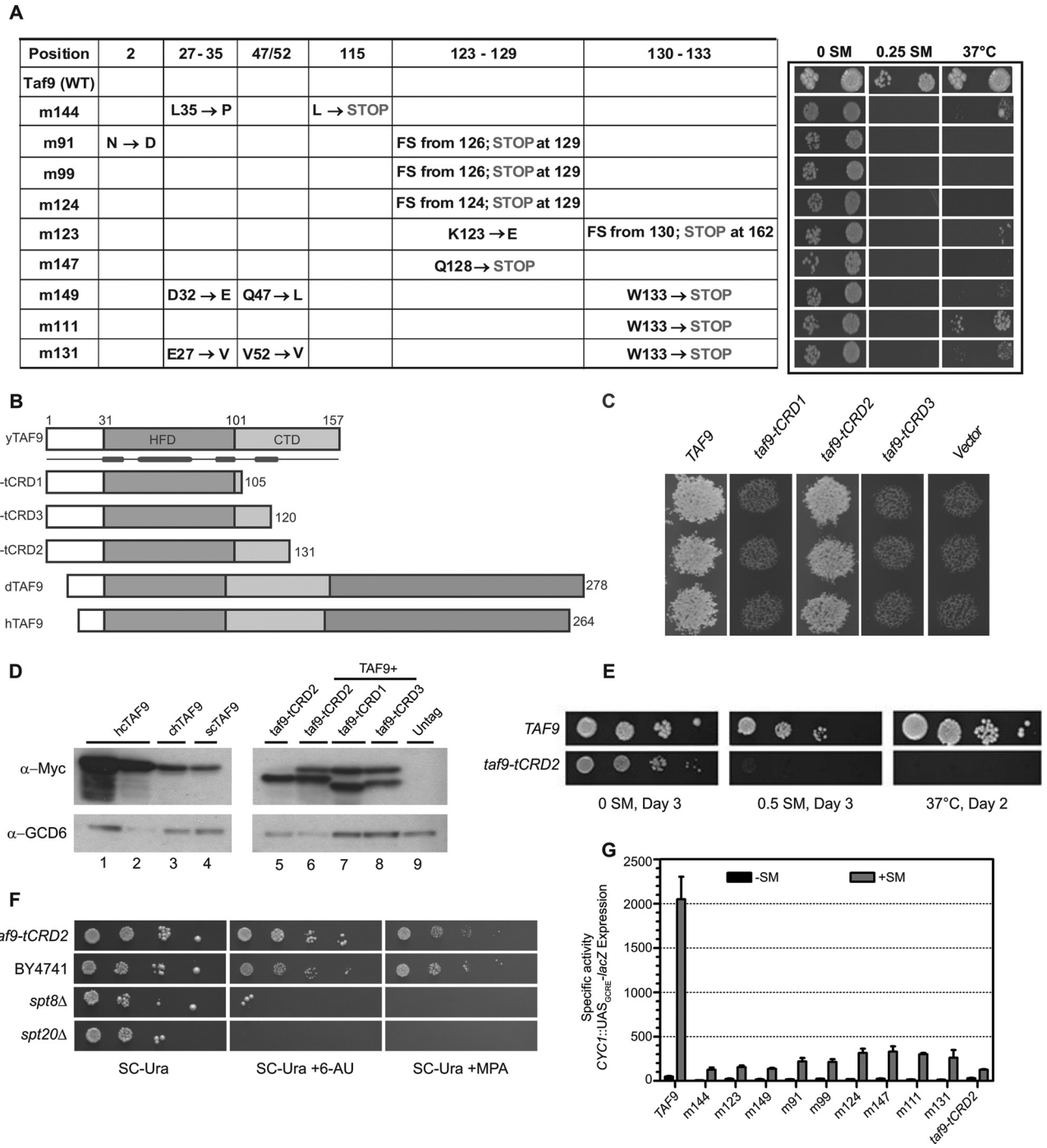

FIG 1 The Taf9 CRD is required for Gcn4-dependent activation. (A) Locations of substitution, frameshift (FS), and nonsense mutations. The SM-sensitive (0.25 μg/ml SM) and temperature-sensitive (37°C) phenotypes are shown on the right. (B) Schematic diagram showing the WT yTaf9 and the Taf9-tCRD1, Taf9-tCRD2, and Taf9-tCRD3 mutant; *Drosophila* (dTaf9); and human (hTaf9) sequences. The evolutionarily conserved histone H3-like HFD and the predicted fourth α-helix (shown as a rectangle below the yTAF9 schematic) in the yTaf9 CRD are shown. The dTaf9 and hTaf9 sequences also contain an additional nonconserved C-terminal extension. (C) Replica print assay of strains RPY72 (*TAF9*), YSS-C4 (*taf9-tCRD1*), YSS-C5 (*taf9-tCRD2*), YSS-C6 (*taf9-tCRD3*), and RPY1 with the YEplac181 vector on SC-Leu plus 5-FOA medium. (D) Western blot of Taf9-Myc_{13} in extracts of RPY67 (lanes 1 and 2; hcTAF9), YSS1 (lane 3; chTAF9), RPY1 (lane 4; scTAF9), or YSS26 (lane 5; Taf9-tCRD2). Lanes 6 to 9 contain extracts from strain RPY1 (scTaf9-Myc_{13}) bearing *taf9-tCRD2* (lane 6), *taf9-tCRD1* (lane 7), or *taf9-tCRD3* (lane 8) or untagged control (lane 9, BY4741). The blot was probed with anti-Myc (α-Myc) antibody or anti-Gcd6 as a control. (E) Spot assay showing the SM-sensitive and temperature-sensitive (Ts^-) phenotypes. The strains were spotted onto SC-Leu-Ile-Val plates with 0.5 μg/ml SM (0.5 SM) or no SM (0 SM) or a YPD plate (37°C). (F) Phenotype test for the transcription elongation defect. The *taf9-tCRD2* strain (RPY101) and control WT (BY4741), *spt8*Δ, and *spt20*Δ strains transformed with vector pRS426 were spotted onto SC-Ura medium alone or onto plates containing 75 μg/ml 6-AU or 15 μg/ml MPA. (G) Reporter assay showing the expression of the *CYC1*::UAS_{GCRE}-*lacZ* fusion in *taf9* mutant strains. The strains were grown in SC-Ura-Leu-Ile-Val medium at 30°C from an OD_{600} of ~0.5, and the cultures were either harvested after 5 h or treated after 2.5 h with 0.5 μg/ml SM and cultured for an additional 6 h. The β-galactosidase specific activity was calculated from six transformants each for non-SM-treated and SM-treated cell extracts. The error bars indicate standard errors of the mean (SEM).

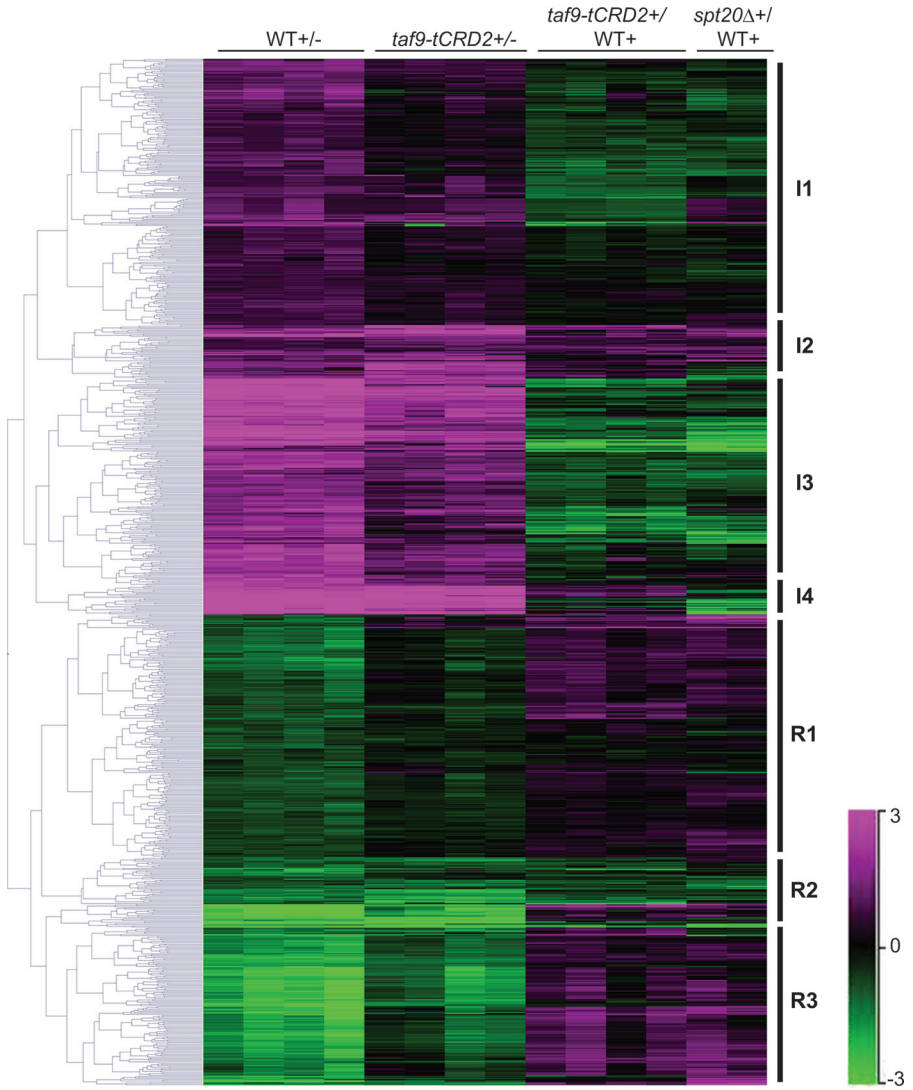

FIG 2 Expression profiles of Taf9 CRD-dependent genes. A hierarchical-cluster map shows the expression of the 963 Taf9 CRD-dependent genes from WT plus SM versus non-SM-treated (WT+/−), *taf9-tCRD2* plus SM versus non-SM-treated (*taf9-tCRD2*+/−), *taf9-tCRD2* plus SM versus WT plus SM (*taf9-tCRD2*+/WT+), and *spt20*Δ plus SM versus WT plus SM (*spt20*Δ+/WT+). The expression profiles of induced (I1 to I4) or repressed (R1 to R3) genes in the WT ± SM data across the different data sets are indicated.

ther substantiated by our analysis of the elongating RNA polymerase II (Rbp1 C-terminal domain [CTD]-Ser2P), discussed below.

We next tested if the *taf9* mutants showed a Gcn4-dependent activation defect using the UAS_{GCRE}::*lacZ* reporter fusion (59). Cell extracts were obtained from WT *TAF9* or the various *taf9* mutants (shown in Fig. 1A) treated or not with SM, and β-galactosidase activity was measured as described previously (48). As expected, the UAS_{GCRE}::*lacZ* reporter was induced ~42-fold in the WT *TAF9* strain upon SM treatment. However, the induction was substantially reduced, by ~10 to 20-fold, in all the mutants, including the *taf9-tCRD2* strain, relative to the control WT *TAF9* strain (Fig. 1G). Thus, the Taf9 CRD is required for transcriptional activation by Gcn4.

Identification of Taf9 CRD-dependent genes. To identify the global requirement of the Taf9 CRD for activation by Gcn4, we conducted microarray analysis using *TAF9* and *taf9-tCRD2* mutant strains with or without SM treatment (see Materials and Methods). To examine the role of the Taf9 CRD for SAGA-regulated transcription, we also performed microarray analysis of the *spt20*Δ mutant (described below). The microarray data revealed that ~17% of yeast genes were Taf9 CRD dependent for their expression, including 463 upregulated genes and 400 downregulated genes. Hierarchical clustering of these Taf9 CRD-dependent genes from all replicate hybridizations yielded seven major gene clusters with altered expression patterns (Fig. 2).

Genes highly induced by SM in the WT strain are in clusters I3 and I4 (Fig. 2), comprising a large number of Gcn4-induced amino-acid-biosynthetic genes identified previously (42). Genes with less induction are in clusters I1 and I2, and the downregulated genes are in clusters R1 to R3 (Fig. 2). A large fraction of the Gcn4-induced amino-acid-biosynthetic genes (42) are in clusters I3 and I4. The Taf9 CRD-dependent genes exhibited two major profiles. The SM-mediated induction of genes in clusters I1 (250 genes) and I3 (194 genes) was either lost (I1) or impaired (I3) in

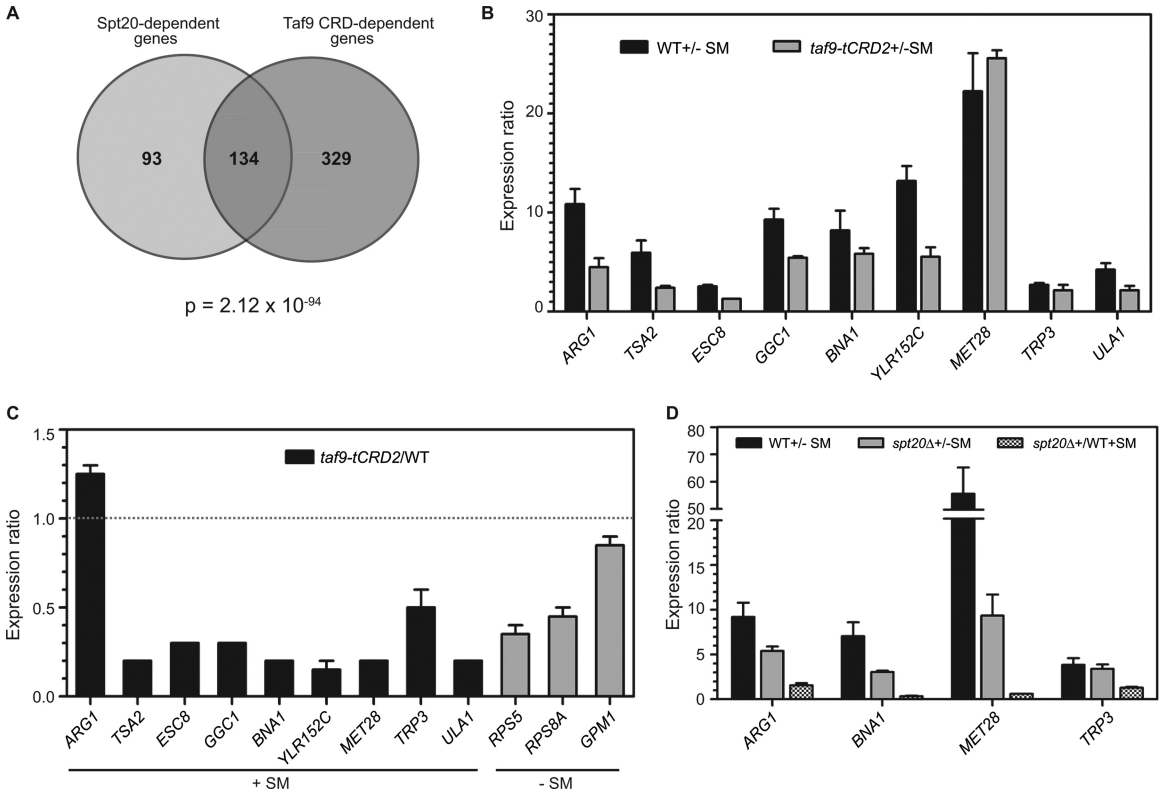

FIG 3 The Taf9 CRD functions in the SAGA pathway for transcriptional activation. (A) Overlap between genes induced in Spt20-dependent and Taf9 CRD-dependent manners at high statistical significance. (B to D) cDNAs from WT (RPY72), *taf9-tCRD2* (YSS26), and *spt20*Δ (number 7390) strains (with or without SM treatment) were used for qRT-PCR analysis using primers for selected genes from cluster I3 (Fig. 2), with *scR1* as an endogenous control, and the results were plotted as the fold induction (B), *taf9-tCRD2* plus SM/WT plus SM ratio (C), or *spt20*Δ plus SM/WT plus SM ratio (D). The expression of *RPS5*, *RPS8A*, and *GPM1* was analyzed under non-SM-treated conditions. The error bars indicate SEM.

the *taf9* mutant relative to the WT strain. These genes included *ALD3*, *ALD4*, *GAP1*, and 14 of the 24 Seripauperin (*PAU*) genes in cluster I1 and *ARG1*, *BNA1*, *MET28*, and *GGC1* from cluster I3, respectively (Fig. 2). Consistent with this result, the same gene clusters were downregulated in the *taf9-tCRD2* plus SM/WT plus SM data (Fig. 2). Although the genes in cluster I4 (27 genes) had comparable SM induction levels in both the WT and the *taf9* mutant, 17 of these genes were downregulated under SM conditions in the *taf9-tCRD2* plus SM/WT plus SM experiment, indicating a Taf9 CRD requirement for expression under SM (Fig. 2).

Paradoxically, other Taf9 CRD-dependent genes (cluster I2) showed greater induction in the *taf9* mutant than in the WT. These 50 genes, including *ILV2*, *MET6*, *MET13*, and *ARO1*, showed equivalent levels of expression in the *taf9*-WT direct comparison (Fig. 2), indicating that their uninduced (non-SM-treated) expression was impaired by the *taf9* mutation. The genes in clusters R1 and R3 are downregulated in a Taf9 CRD-dependent manner, as their repression is either lost (R1) or impaired (R3) in the *taf9* mutant. Genes in R2 showed greater repression in the *taf9* mutant than in the WT strain (Fig. 2). Together, these data revealed that the Taf9 CRD is required for genome-wide transcription of a large number of genes and impacts transcription in multiple ways.

Taf9 CRD functions in the SAGA pathway. Next, we determined the relationship between the Taf9 CRD and SAGA for genome-wide expression under amino acid starvation conditions. Although SAGA-regulated genes have been identified by profiling an *spt3*Δ mutant (15), no data on the genome-wide requirement for SAGA under SM conditions is available. Therefore, we carried out microarray profiling of the WT and the *spt20*Δ mutant strains under SM conditions. A total of 974 genes (~17% of the genome) were differentially regulated (up- or downregulated by1.5-fold in *spt20*Δ and the WT strains), including 555 and 419 genes that required Spt20 for their upregulation ($\log_2 \leq -0.585$ in *spt20*Δ and WT strains) or downregulation ($\log_2 \geq 0.585$ in *spt20*Δ and WT strains), respectively. In the WT ± SM data, 227 of the above-mentioned 555 genes were upregulated, implying that the genes require Spt20 for their induction in SM. Of the 419 genes with elevated expression in the *spt20*Δ mutant, 105 genes were also downregulated in the WT ± SM data, suggesting Spt20-dependent repression.

We next analyzed the overlap between genes induced in the Taf9 CRD and Spt20 data sets and found a statistically significant overlap between genes induced in a manner dependent on both the Taf9 CRD and Spt20 (Fig. 3A). Thus, a common set of 134 genes are dependent on the Taf9 CRD and Spt20, suggesting that the Taf9 CRD functions in the SAGA pathway of transcriptional activation. The rest of the Taf9 CRD-induced genes were not impaired by the *spt20*Δ mutation, suggesting that the Taf9 CRD also functions outside the Spt20/SAGA pathway for transcriptional activation.

Next, we examined the expression of selected Taf9 CRD-de-

pendent genes using qRT-PCR analysis. The magnitude of induction by SM in the WT strain ranged between 2- and 25-fold (Fig. 3B). In the *taf9* mutant strain, induction was impaired for all genes except *MET28* and *TRP3* (Fig. 3B). When the relative expression levels between the WT and the *taf9* mutant in SM medium (*taf9-tCRD2* plus SM/WT plus SM) were compared, transcription of *MET28* and *TRP3* was also found to be Taf9 CRD dependent (Fig. 3C). Although induction of *ARG1* mRNA by SM was impaired in the *taf9* mutant (~4-fold compared to ~10-fold in the WT) (Fig. 3B), the *ARG1* mRNA level was not reduced in the mutant in SM medium (Fig. 3C), as was also reported for the *gcn5*Δ, *spt3*Δ, and *spt8*Δ mutants (44). As the *ARG1* mRNA level in non-SM-treated medium was slightly elevated (ΔC_T values) (data not shown), this could partly dampen the perceived induction, indicating that activation of *ARG1* transcription was not substantially impaired by the Taf9 CRD mutation. Although *RPS5*, *RPS8A*, and *GPM1* were not in our list of Taf9 CRD-dependent genes, we also examined the expression of *RPS5* and *RPS8A*, shown previously to be Taf (TFIID) dependent (18, 19, 60, 61), and *GPM1*, shown to be TFIID independent (29) under SM-free conditions. Indeed the mRNA levels of the two RP genes, but not that of *GPM1*, were reduced in the *taf9* mutant strain relative to that of the WT (Fig. 3C). Together, the qRT-PCR data showed that the transcriptional activation of several genes was dependent on the Taf9 CRD.

To validate the Spt20 requirement for transcriptional activation, we carried out qRT-PCR analysis of the selected genes *BNA1*, *MET28*, and *TRP3* and included the previously studied *ARG1*, which was shown to be bound by SAGA, as well as SAGA dependent for activation (46). Our qRT-PCR data showed that the induction by SM of *ARG1*, *BNA1*, and *MET28* mRNAs, but not that of *TRP3*, was impaired in the *spt20*Δ mutant (Fig. 3D). Together, the expression analyses discussed above revealed that genes induced in a Taf9 CRD-dependent manner comprise those induced by Gcn4 and also include both Spt20/SAGA-dependent and -independent genes.

Taf9 CRD-dependent genes are regulated by Gcn4 and several other activators. To gain further insights into the Taf9 CRD requirement for transcriptional activation by Gcn4 and other TFs, we examined the Taf9 CRD-induced gene promoters for the occupancy of TFs studied under SM conditions in a ChIP-on-chip study by the Young laboratory (62). We asked what fraction of the promoters bound by each of the 34 TFs (at P values of ≤0.01 and ≤0.005) showed Ta9 CRD dependence and found that the vast majority of the TFs were bound to one or more of the Taf9 CRD gene promoters (see Tables S4 and S5 in the supplemental material). Of these TFs, only Gcn4, Arg81, and Cad1/Yap2 were bound significantly ($P < 0.05$) more to the Taf9 CRD-dependent genes than expected relative to the negative gene set (see the supplemental material; also, data not shown). Since not all TFs were studied by Harbison et al. under amino acid starvation conditions, the requirement for the Taf9 CRD, if any, could not be predicted for such TFs. Our analysis suggests that multiple TFs, as demonstrated here for Gcn4, could require the Taf9 CRD for their transcriptional activation.

Next, we asked how many of the 463 Taf9 CRD-induced genes were represented among the 515 Gcn4-induced genes identified previously (42). The Venn diagram yielded 175 genes (~34%) that overlapped between the two gene sets, and this overlap was highly significant (Fig. 4A). To validate the requirement for Gcn4 for the expression of Taf9 CRD-dependent genes, we carried out qRT-PCR analysis for the expression of selected genes from among the 175 genes dependent on both the Taf9 CRD and Gcn4 for their induction (Fig. 4A). The data showed that the expression of *ARG1*, *TSA2*, *ESC8*, *GGC1*, *BNA1*, *YLR152C*, *MET28*, and *TRP3* was induced in SM medium but was highly impaired in the *gcn4*Δ mutant (Fig. 4B). The expression of *ULA1*, although Taf9 CRD dependent (Fig. 3B and C), was not known to be Gcn4 dependent previously (42), and our qRT-PCR data confirmed that *ULA1* expression was not impaired in the *gcn4*Δ mutant (Fig. 4B). Together, these results indicate that SM-inducible Taf9 CRD-dependent genes include both Gcn4-independent and -dependent genes.

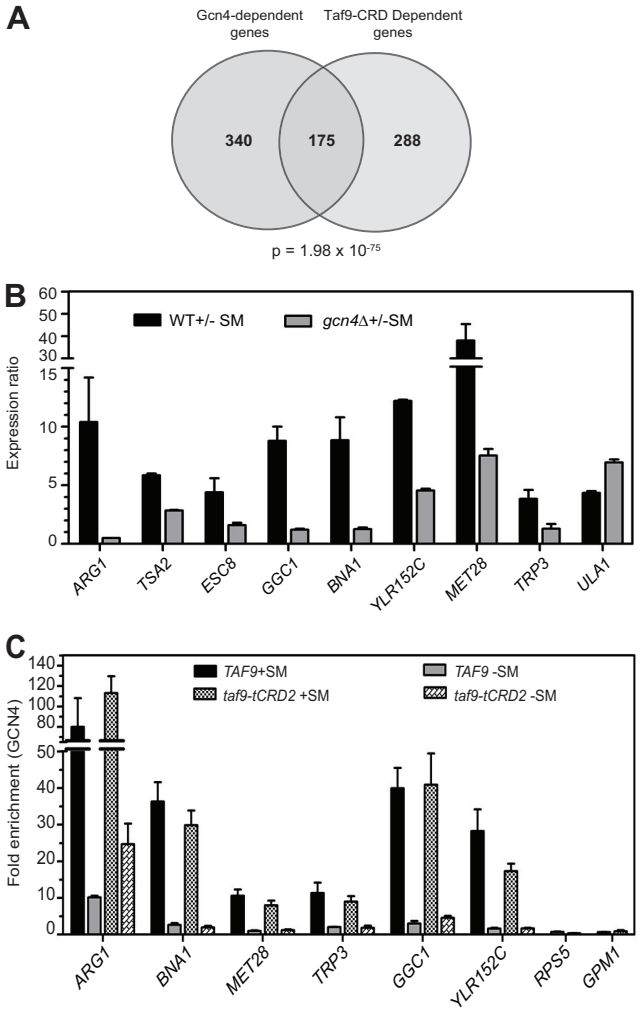

FIG 4 Gcn4-mediated activation of Taf9 CRD-dependent genes. (A) Venn diagram showing statistically significant overlap between genes induced in Taf9 CRD-dependent (463 genes; this study) and Gcn4-dependent (515 genes [42]) manners. (B) qRT-PCR validation of genes from cluster I3 (Fig. 2) to determine Gcn4 dependence for activation. cDNA was prepared from total RNA isolated from WT (RPY72) and *gcn4*Δ (strain 249) strains (with or without SM) and analyzed as for Fig. 3B. (C) Recruitment of Gcn4 in the UAS regions of Taf9 CRD-dependent genes. Cross-linked chromatin extracts from the WT *TAF9* (YMS94) or *taf9-tCRD2* (YMS95) strain treated or not with SM were used to immunoprecipitate Gcn4 using 5 μl polyclonal anti-Gcn4 antibody per IP reaction. The fold enrichment was calculated relative to the *POL1* ORF as a control. The error bars indicate SEM from a minimum of two chromatins and three IP reactions.

A large fraction of genes identified in this study as dependent on Gcn4 and the Taf9 CRD have not been previously demonstrated to be bound by Gcn4 at their promoters. Therefore, a limited number of Taf9 CRD-dependent genes reported to be bound by Gcn4 in SM medium in the ChIP-on-chip study (62) were selected, and ChIP assays were conducted to determine Gcn4 occupancy in SC medium with or without SM. Indeed, the ChIP data showed increased Gcn4 occupancy in the upstream promoter regions of *ARG1*, *BNA1*, *MET28*, *TRP3*, *GGC1*, and *YLR152C* gene promoters in the WT strain in SM medium (Fig. 4C). On the other hand, no Gcn4 enrichment was obtained at the *RPS5* and *GPM1* promoters. Importantly, the ChIP data showed that Gcn4 occupancy was not compromised at these promoters, except for a slight reduction at *YLR152C*, in the *taf9* mutant strain (Fig. 4C).

The TAF9 CRD mutant can interact with full-length TAF6. We next tried to ascertain the cause of the Taf9 CRD-dependent activation defect. It is possible that the *taf9-tCRD2* phenotype resulted from a heterodimerization defect between Taf9 and Taf6. Although Taf9-Taf6 interaction at a minimum requires the HF domains (30), it is not clear if additional sequence determinants are required for Taf9-Taf6 interaction in a full-length context. Therefore, we carried out pulldown assays using GST-Taf6 and MBP fusions bearing the WT or the mutant Taf9-tCRD1 and -tCRD2 proteins. The pulldown data showed that truncated Taf9 can interact with full-length Taf6, although at slightly reduced levels compared to the WT (see Fig. S2 in the supplemental material). We also examined the interaction of the Taf9 CRD with Taf6 *in vivo* using a dominant-negative genetic assay. We reasoned that overexpression of truncated Taf9 mutant proteins could squelch Taf6, leading to a dominant-negative growth defect. Yeast strain BY4741 was transformed with high-copy-number plasmids expressing Myc_{13}-tagged *TAF9*; *taf9-tCRD1*, *-tCRD2*, *-tCRD3*; or the empty vector YEplac181, and the SM-sensitive phenotype was examined. Indeed, overexpression of all three truncation mutants caused SM-sensitive growth defects (Fig. 5A). Western blot analysis showed that the mutant constructs were indeed overexpressed in these strains compared to single-copy WT Taf9 (Fig. 5B). Together, these data showed that the Taf9 truncation mutants retained their ability to interact with Taf6 both *in vitro* and *in vivo*.

TFIID and SAGA integrity is largely intact in the Taf9 CRD mutant cell extract. We next examined the stability of Taf9-containing SAGA and TFIID complexes in the *taf9* mutant strain. Myc_{13}-tagged *TAF11*, a TFIID-specific subunit, or *SPT7*, a SAGA-specific subunit, was coimmunoprecipitated from the *TAF9-HA*$_3$ or *taf9-tCRD2-HA*$_3$ strain. The Taf11-Myc_{13} immunoprecipitation led to the pulldown of the TFIID subunits Taf1 and TBP and the shared TAF subunits Taf12, Taf5, Taf6, and Taf9 from WT and *taf9* mutant cell extracts (Fig. 5C). Moreover, the Spt7-Myc_{13} immunoprecipitation led to the pulldown of Gcn5, Tra1, and the shared TAF subunits Taf12, Taf5, Taf6, and Taf9 from the WT and *taf9* mutant cell extracts (Fig. 5D). Snf6, a SWI/SNF subunit, and TBP did not coprecipitate with Spt7-Myc_{13}. In both TFIID and SAGA coimmunoprecipitations, the recovery of Taf9-tCRD2, and Taf6 and Taf5 to a lesser extent, was slightly reduced in the mutant compared to that from the WT. Together, these coimmunoprecipitation assays demonstrated that Taf9-tCRD2 could associate with TFIID and SAGA complexes in cell extracts.

Gcn4 interaction with SAGA is intact in the Taf9 CRD mutant. Previous studies have shown that SAGA interaction with the Gcn4 activation domain is mediated by Tra1 (51, 63) and Taf12 subunits (48, 63). Moreover, these subunits are also required for transcriptional activation of target genes by Gcn4, thereby providing physical and functional interaction of SAGA subunits with Gcn4. Therefore, we tested whether the lack of the Taf9 CRD impaired the interaction of Gcn4 with the SAGA complex. GST pulldown assays (9, 23) using GST-Gcn4 showed interaction of Spt7, Gcn5, Tra1, Taf12, and Taf9 from the *TAF9-HA*$_3$ extract in a manner dependent on the WT Gcn4 activation domain (Fig. 5E). As expected from our previous study (9), the SWI/SNF subunit Snf6, used as a control here, was specifically pulled down. Whereas no interaction with Taf1 was seen, interaction with TBP did not show specificity for the Gcn4 activation domain, as observed previously (9, 23). The pulldown assays conducted from the *tCRD2-HA*$_3$ extract also showed the pulldown of the same SAGA subunits, albeit with reduced recovery of the Gcn5 subunit (Fig. 5E). Importantly, the interaction of Gcn4 with Tra1 and Taf12 was not impaired in the *tCRD2-HA*$_3$ extract (Fig. 5E). Together, these results indicate that the interactions of the Gcn4 activation domain with the mutant SAGA complex are largely intact *in vitro*.

Taf9 recruitment to promoters is dependent on the Taf9 CRD. We next assessed the requirement for the Taf9 CRD for promoter recruitment of Taf9 *in vivo*. For ChIP analysis, we selected the *ARG1*, *BNA1*, *MET28*, *TRP3*, and *RPS5* genes, which showed Taf9 CRD dependence for expression along with *GPM1*, whose expression was not impaired by the *taf9* mutation (Fig. 3). In WT cells, Taf9 occupancy at the *ARG1* locus, well studied as a model for Gcn4-mediated recruitment of coactivators and PIC (7, 45, 46), was highly enriched in the *ARG1*$_{UAS}$, *ARG1*$_{core}$, and *ARG1* 5′ ORF regions under SM-treated versus non-SM-treated conditions (Fig. 6A). However, Taf9-tCRD2 occupancy was reduced to background levels at these locations under SM-treated conditions, except in the *ARG1* 3′ ORF region (Fig. 6A).

ChIP data also showed that Taf9 occupancy was substantially enriched above background in the Gcn4-dependent *BNA1*$_{UAS}$, *BNA1*$_{core}$, *TRP3*$_{UAS}$, *TRP3*$_{core}$, and *MET28*$_{core}$ promoter regions and was induced in SM-treated versus non-SM-treated medium, except at *BNA1*$_{UAS}$, where no SM-induced stimulation was seen (Fig. 6B). Our data also showed that Taf9 occupancy was CRD dependent at the UAS and core promoter of *RPS5* and the *GPM1*$_{core}$ promoter under non-SM-treated conditions (Fig. 6B). Together, these data demonstrated a strong requirement for the Taf9 CRD for Taf9 occupancy at both Gcn4-dependent and Gcn4-independent promoters *in vivo*.

The Taf9 CRD is required for SAGA recruitment. We next studied Spt7-Myc_{13} recruitment at the *ARG1* locus in *TAF9* and *taf9-tCRD2* strains. Spt7 occupancy was strongly stimulated at the *ARG1*$_{UAS}$ in the WT strain under SM-treated compared to non-SM-treated conditions (Fig. 6C), and the induction was completely abolished by the *taf9-tCRD2* mutation. Spt7 occupancy was induced between 2- and 4-fold at the *ARG1*$_{core}$, 5′ ORF and 3′ ORF regions in SM in the WT strain but was abrogated by the *taf9-tCRD2* mutation, except at the *ARG1* 3′ ORF (Fig. 6C). Gcn5, as part of SAGA, promotes histone H3 K9/14 acetylation at the *ARG1* locus (45). We tested if the defective SAGA recruitment could reduce acetylation in the *taf9* mutant. Indeed, H3 K9/14Ac levels were reduced across the *ARG1* locus in the mutant in comparison to the WT (Fig. 6D). In the 3′ ORF region, although Spt7/SAGA occupancy was stimulated by SM, the H3 K9/14Ac level was not high enough compared to other regions in the WT (Fig. 6C and D), probably because of the recruitment of multiple deacetylases to

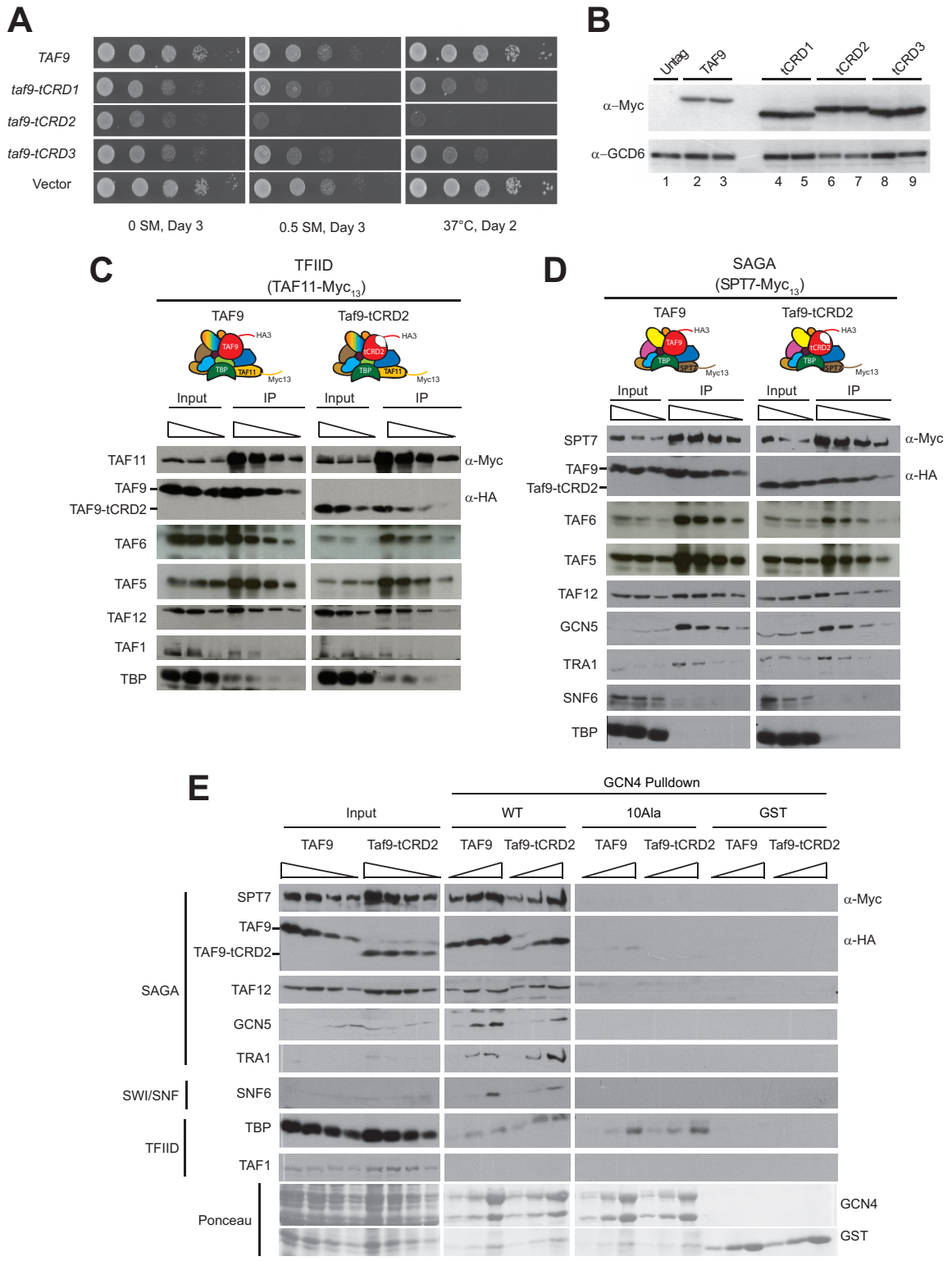

FIG 5 Truncation of the Taf9 CRD does not impair TAF6-TAF9 interaction, SAGA/TFIID complex stability, or Gcn4-SAGA interaction. (A and B) Dominant-negative phenotype and Western blot analysis. (A) Strain BY4741 transformed with *TAF9-Myc*$_{13}$ (YMS147), *taf9-tCRD1*(YMS28), *taf9-tCRD2* (YMS30), and *taf9-tCRD3* (YMS34), or control empty vector YEplac181 (YMS27) was spotted onto SC-Leu plates with no SM or 0.5 μg/ml SM and incubated at 30°C or on a YPD plate at 37°C. (B) Western blot analysis showing overexpression of tCRD1 (lanes 4 and 5), tCRD2 (lanes 6 and 7), and tCRD3 (lanes 8 and 9). The untagged control (lane 1) and WT Taf9 control (lanes 2 and 3) are also shown. (C and D) Coimmunoprecipitation of Taf11-Myc$_{13}$ from the YMS14 (TAF9) and YMS16 (Taf9-tCRD2) strains (C) and Spt7-Myc$_{13}$ from the YMS10 (TAF9) and YMS11 (Taf9-tCRD2) strains (D), using anti-Myc antibody. Serial dilutions containing 50 μg, 25 μg, and 12.5 μg of the input extracts or 2-fold serial dilutions of the immunoprecipitates were denatured, resolved through 6 to 12% SDS-PAGE, blotted onto a Hybond ECL membrane, and probed with the indicated antibodies. (E) GST-Gcn4 interaction with SAGA. Yeast whole-cell extracts from *TAF9* and *taf9-tCRD2* strains shown in panel C were used for pulldown analysis from *Escherichia coli* lysates containing either WT GST-Gcn4 (p2528), the 10 Ala mutant (p2144), or empty vector (GST). Three concentrations of each GST protein were mixed with 1 mg yeast cell extracts, incubated on ice for 1 h, clarified, and pulled down with glutathione (GSH)-Sepharose beads. The input lanes were loaded with 120 μg cell extracts and 2-fold serial dilutions and the pulldown lanes with 2-fold serial dilutions of the eluates and analyzed as described for panels B and C. The Ponceau S-stained blots are also shown.

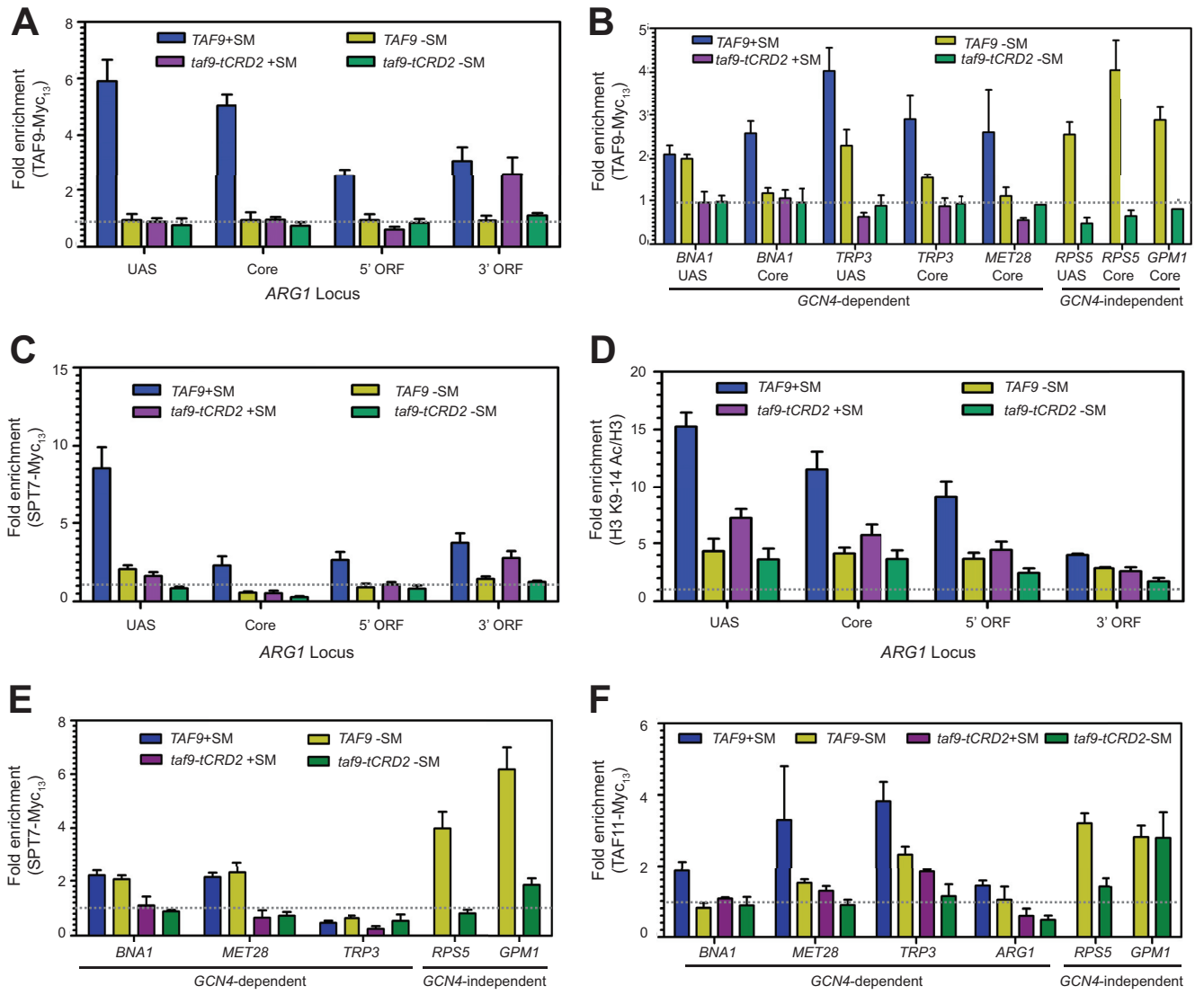

FIG 6 The Taf9 CRD is required for occupancy of Taf9 complexes *in vivo*. (A and B) Occupancy of Myc_{13}-tagged Taf9 and Taf9-tCRD2 at the *ARG1* locus under SM-treated and untreated conditions (A) and occupancy at other Gcn4-dependent promoters under SM-treated and untreated conditions or at Gcn4-independent promoters *RPS5* and *GPM1* under non-SM-treated conditions (B). (C) Occupancy of Spt7-Myc_{13} at the *ARG1* locus in *TAF9* and *taf9-tCRD2* strains under SM-treated and untreated conditions. (D) Levels of histone H3 K9/14Ac at the *ARG1* locus under SM-treated and untreated conditions. A ChIP assay was done with anti-H3 K9/14Ac antibody and normalized to the total histone H3 level by immunoprecipitation with pan-anti-H3 antibody. (E) Spt7-Myc_{13} occupancy in *TAF9* and *taf9-tCRD2* strains in the UAS regions of the Gcn4-dependent promoters under SM-treated and untreated conditions or in the $RPS5_{UAS}$ and upstream region of *GPM1* under non-SM-treated conditions. (F) Core promoter occupancy of Taf11-Myc_{13} at Gcn4-dependent targets in *TAF9* and *taf9-tCRD2* strains under SM-treated and untreated conditions or at *RPS5* and *GPM1* under non-SM-treated conditions. The *POL1* coding sequence was used as a nonspecific control, except in panel D, where the TEL06R-XC region was used. For each analysis, enrichment values were obtained from 3 or 4 chromatin immunoprecipitation assays from at least two independent chromatin preparations. The error bars indicate SEM.

the *ARG1* 3′ ORF region, as reported previously (45). Together, our results showed that the Taf9 CRD is required for SAGA recruitment and SAGA-mediated H3 K9/14Ac at the *ARG1* locus.

We also examined Spt7/SAGA occupancy in the UAS regions of the *BNA1*, *MET28*, *TRP3*, *RPS5*, and *GPM1* promoters. The Spt7-Myc13 occupancy, although not induced by SM in the *BNA1* and *MET28* UAS regions, was higher than background levels (Fig. 6E), but this enrichment was abolished in the mutant (Fig. 6E). No specific enrichment of Spt7/SAGA was found in the $TRP3_{UAS}$ region, consistent with *TRP3* being a TFIID target (15, 18). Wild-type *TAF9* strains showed high Spt7 occupancy in the *GPM1* (upstream) and $RPS5_{UAS}$ regions under non-SM-treated conditions, which was almost abolished in the *taf9* mutant (Fig. 6E). Two previous reports have examined SAGA occupancy at RP gene promoters (64, 65). Whereas Bhaumik and Green (64) reported no enrichment of SAGA, Ohtsuki et al. (65) carried out ChIP-on-chip and reported enrichment of the Gcn5 subunit for several RP gene promoters. Together, our results demonstrate that SAGA recruitment to multiple promoters is dependent on the Taf9 CRD.

TFIID recruitment to multiple TAF-dependent promoters requires the Taf9 CRD. To examine the requirement for the Taf9 CRD for TFIID recruitment, *TAF11-Myc*$_{13}$ occupancy was exam-

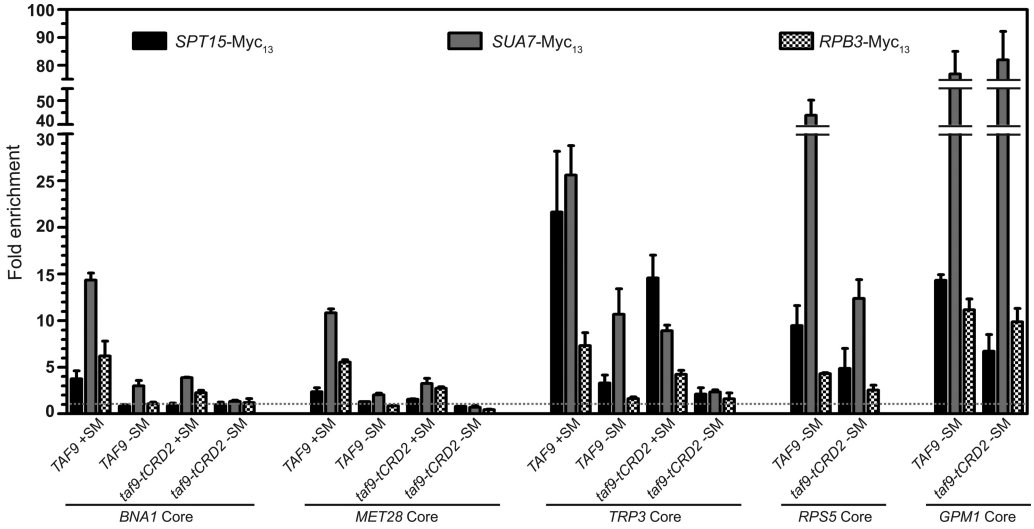

FIG 7 Requirement for Taf9 CRD for PIC assembly. Recruitment of Spt15-Myc$_{13}$ (TBP), Sua7-Myc$_{13}$ (TFIIB), and Rpb3-Myc$_{13}$ (RNAP II) was determined at the core promoters of Gcn4-dependent *BNA1*, *TRP3*, and *MET28* genes under SM- and non-SM-treated conditions, as well as at the Gcn4-independent *RPS5* and *GPM1* core promoters under non-SM-treated conditions, by ChIP assays using anti-Myc antibody. For each analysis, enrichment values were obtained with reference to a nonspecific *POL1* coding sequence probe. Data from three chromatin immunoprecipitation assays from at least two independent chromatin preparations are plotted. The error bars indicate SEM.

ined in *TAF9* and *taf9-tCRD2* mutant strains. In the Gcn4-regulated core promoter regions of *BNA1*, *MET28*, and *TRP3*, the Taf11-Myc$_{13}$ occupancy was induced ~2 to 4-fold under SM-treated conditions compared to SM-free conditions in the *TAF9* strain (Fig. 6F), which was severely impaired in the *taf9* mutant, indicating Taf9 CRD dependence for TFIID occupancy. At the *ARG1*$_{core}$ promoter, however, little or no Taf11-Myc$_{13}$ occupancy was enriched in the WT strain treated with SM (Fig. 6F). At the Gcn4-independent *RPS5*$_{core}$ promoter, as expected from previous studies on other TFIID subunits (18, 19, 60), the *TAF11-Myc*$_{13}$ subunit occupancy was enriched at this locus in the WT but was completely lost in the *taf9* mutant (Fig. 6F), indicating the impairment of TFIID occupancy by the Taf9 CRD mutation. At the *GPM1*$_{core}$ promoter, we obtained ~3-fold enrichment of *TAF11-Myc*$_{13}$ occupancy above background that was unaffected by the Taf9 CRD mutation, indicating Taf9 CRD-independent TFIID recruitment at the *GPM1*$_{core}$ promoter (Fig. 6F). Thus, at multiple Gcn4-dependent core promoters and the Gcn4-independent *RPS5*$_{core}$ promoter, the Taf9 CRD is required for TFIID occupancy.

PIC assembly at several promoters is dependent on the Taf9 CRD. To investigate if the SAGA/TFIID occupancy defects led to a concomitant defect in assembly of the preinitiation complex, we carried out ChIP assays using *SPT15-Myc*$_{13}$ (TBP)-, *SUA7-Myc*$_{13}$ (TFIIB)-, and *RPB3-Myc*$_{13}$ (RNAP II)-tagged strains bearing *TAF9* or *taf9-tCRD2* alleles. The ChIP data showed that the occupancy of TBP, TFIIB, and RNAP II was highly stimulated under SM-treated conditions in the *TAF9* strain relative to non-SM-treated conditions in the *BNA1*, *MET28*, *TRP3*, and *ARG1* core promoter regions (Fig. 7 and 8B). Thus, amino acid starvation conditions elicited by SM treatment led to stimulation of PIC assembly at multiple promoters regulated by Gcn4, consistent with previous data on PIC assembly at the *ARG1* core promoter (8, 45). The PIC assembly at the Gcn4-independent *RPS5* and *GPM1* core promoters was also highly enriched in the *TAF9* strain under non-SM-treated conditions (Fig. 7).

Next, we examined the occupancy of TBP at each of these promoters in the *taf9* mutant strain and found that TBP occupancy was reduced to background levels at *BNA1* and *MET28* in the mutant (Fig. 7). However, at the *TRP3*, *RPS5*, and *GPM1* (Fig. 7) and the *ARG1* (Fig. 8B) core promoters, TBP occupancy was reduced but not abolished. Thus, the Taf9 CRD was required for TBP recruitment at all core promoters examined. The ChIP data also showed that both TFIIB and RNAP II occupancy was substantially impaired at the *BNA1*, *MET28*, *TRP3*, and *RPS5* core promoters in the mutant. At the *GPM1*$_{core}$ promoter, however, the occupancy of TFIIB and RNAP II was unaffected in the *taf9* mutant (Fig. 7), consistent with the WT level of *GPM1* mRNA in the mutant (Fig. 3C).

PIC assembly occurs despite the absence of the Taf9 CRD at the *ARG1* core promoter. As discussed previously, although SAGA occupancy at *ARG1* was highly Taf9 CRD dependent, *ARG1* transcription was not highly dependent on the Taf9 CRD (Fig. 3B and C). To probe this, we examined the occupancy of the mediator, TBP, TFIIB, and RNAP II at the *ARG1* locus in detail using ChIP assays. The mediator (Gal11-Myc$_{13}$) occupancy at *ARG1*$_{UAS}$ was stimulated upon SM addition in WT cells (Fig. 8A). Unexpectedly, Gal11-Myc$_{13}$ occupancy was elevated under both non-SM-treated and SM-treated conditions in the *taf9* mutant strain (Fig. 8A). The occupancy of TBP (Spt15-Myc$_{13}$), TFIIB (Sua7-Myc$_{13}$), and RNAP II (Rpb3-Myc$_{13}$ and Rpb1) was induced at *ARG1*$_{core}$ under SM-treated conditions in the WT strain and was not compromised in the *taf9* mutant strain (Fig. 8B and C).

We next tested if the form of RNAP II recruited to the *ARG1* locus is active in elongation by measuring the Rpb1 CTD-Ser2P levels, a hallmark of elongating RNAP II (reviewed in reference 66). The ChIP data showed increasing Rpb1 CTD-Ser2P levels from the *ARG1*$_{core}$ through the body of the gene in the WT *TAF9* strain in a manner induced by SM treatment (Fig. 8C). These levels were further elevated in the *taf9* mutant under SM-treated conditions (Fig. 8C), indicating that Taf9 CRD mutation causes increased RNAP II elongation in the *ARG1* coding sequence. The

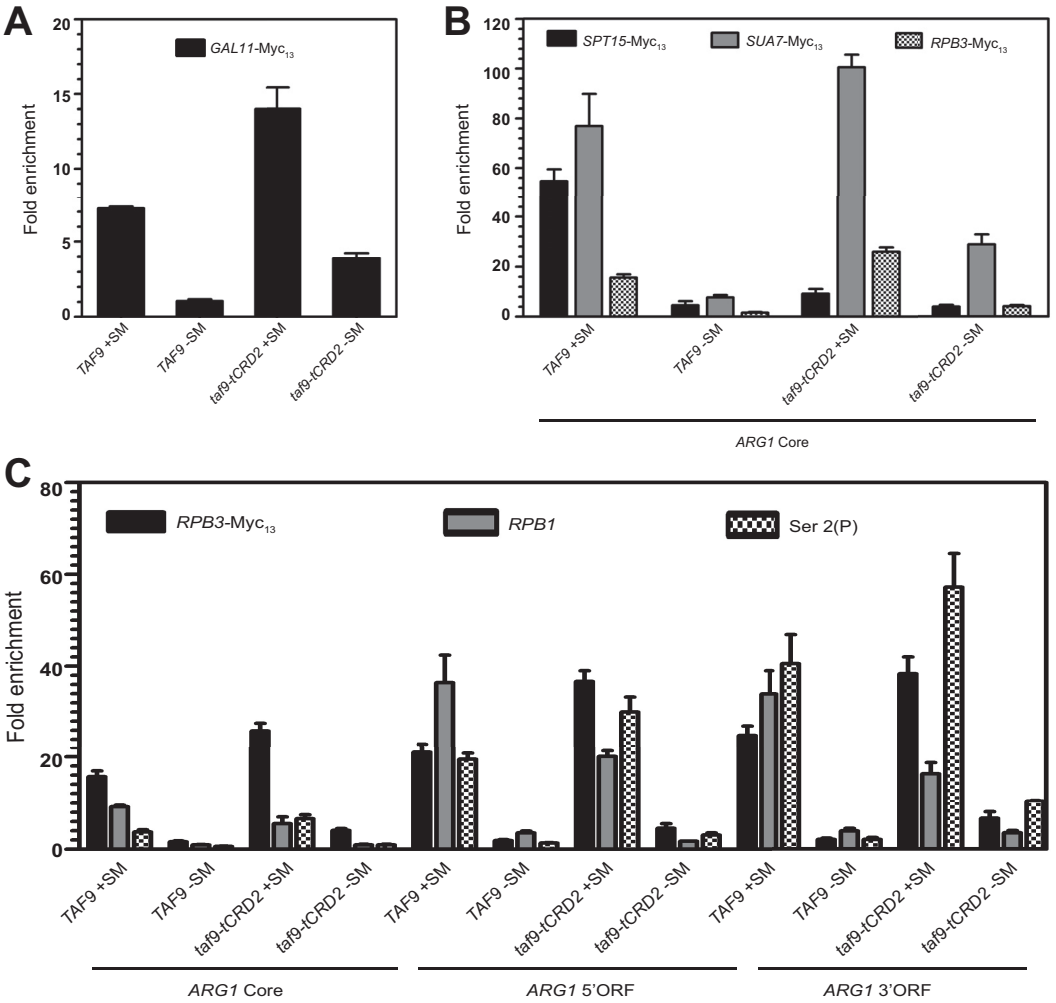

FIG 8 Taf9 CRD-independent PIC assembly at the *ARG1* locus. (A) Mediator recruitment was analyzed at $ARG1_{UAS}$ using Gal11-Myc_{13}. (B) Recruitment analysis of Spt15-Myc_{13} (TBP), Sua7-Myc_{13} (TFIIB), and Rpb3-Myc_{13} (RNAP II) at the $ARG1_{core}$ promoter. (C) Analysis of Rpb1-Ser2(P) levels across the *ARG1* locus. ChIP assays were performed using chromatin extracts from tagged strains in *TAF9* and *taf9-tCRD2* strain (with or without SM) backgrounds. Anti-Myc, 8WG16 (unphosphorylated Rpb1), or anti-Ser2P antibodies were used for ChIP analysis, with a probe corresponding to the *POL1* coding sequence as a nonspecific control. The normalized data were obtained from 3 or 4 chromatin immunoprecipitation assays from at least two independent chromatin preparations. The error bars indicate SEM.

elevated Gcn4 level at the $ARG1_{UAS}$ (Fig. 4C) is perhaps responsible for enhanced mediator recruitment, which could in turn contribute to RNAP II delivery to the $ARG1_{core}$ promoter in the *taf9* mutant (Fig. 8C). These results are also consistent with SAGA-independent mediator recruitment by Gcn4 at the $ARG1_{UAS}$ (7). We suspect that the level of TBP, although reduced, could be sufficient to promote robust PIC assembly at the $ARG1_{core}$ promoter.

DISCUSSION

The Taf9 CRD is required for Gcn4- and SAGA-dependent transcriptional activation and for genome-wide transcription. In this study, using an unbiased genetic screen combined with genetic and biochemical analyses, we determined that the evolutionarily conserved Taf9 C-terminal region is a critical domain required for transcriptional activation by Gcn4 and other activators. The C-terminal truncation of the Taf9 CRD resulted in SM-sensitive and heat-sensitive growth phenotypes (Fig. 1A) and reduced Gcn4-dependent transcriptional activation of multiple Gcn4 target genes, including that of a Gcn4-dependent reporter $CYC1_{GCRE}$-*lacZ* gene construct (Fig. 1G).

Genome-wide transcriptome analysis conducted under Gcn4-activating conditions showed that a large fraction of yeast genes were Taf9 CRD dependent, including ~463 upregulated and ~400 downregulated genes (Fig. 2). Interestingly, at least 34% of the Taf9 CRD-dependent genes (Fig. 4A) were previously shown to be activated by Gcn4 (42). Moreover, our analysis of previous ChIP-on-chip data for 34 transcriptional regulators studied by the Young laboratory (62) revealed that Gcn4, in addition to other TFs, was bound under SM conditions to the Taf9 CRD gene promoters. These analyses indicated a requirement for the Taf9 CRD for promoter activation by multiple transcriptional regulators.

The Taf9 CRD-dependent genes included both SAGA- and TFIID-dependent genes identified in other studies (15–17, 67). Transcriptome profiling of a *spt20*Δ mutant under amino acid starvation conditions showed that almost 60% of the SAGA-de-

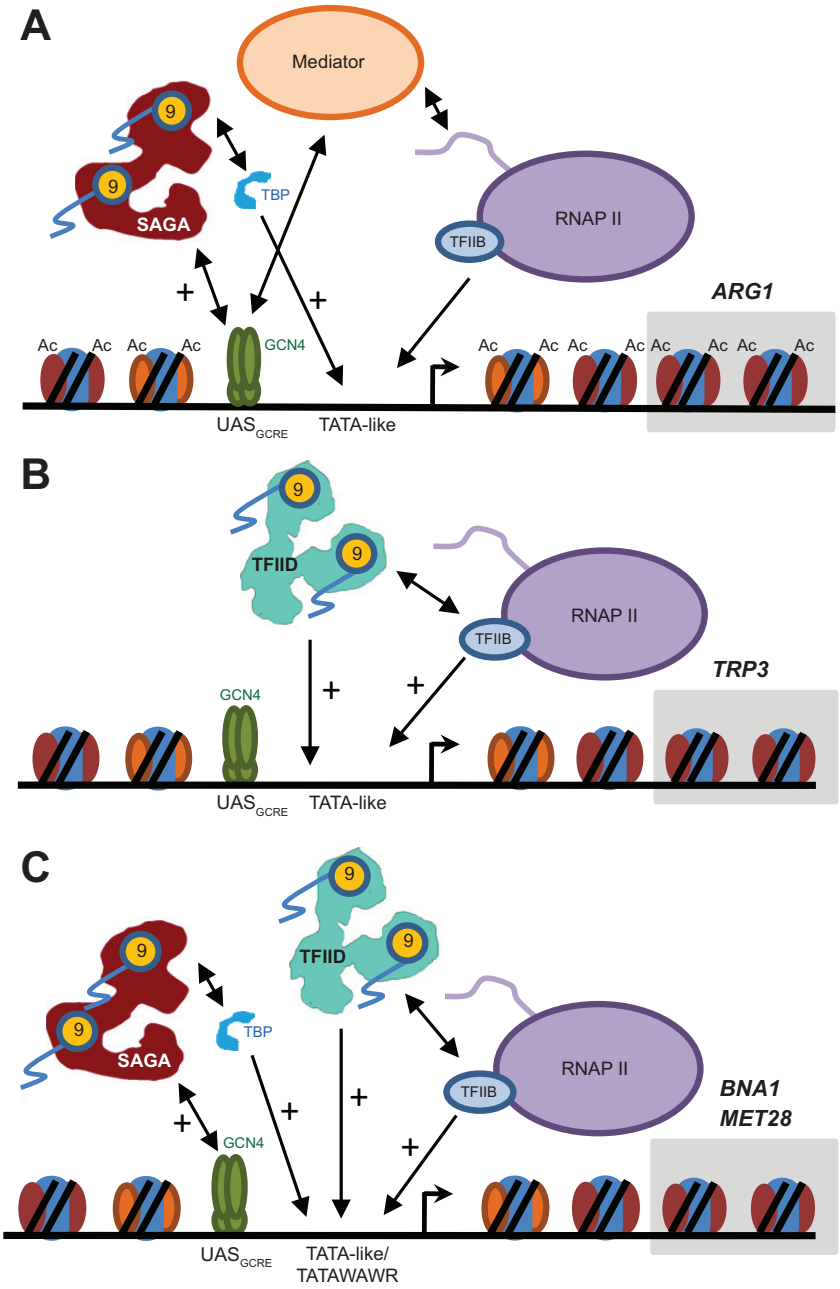

FIG 9 Taf9 CRD is required for coactivator occupancy, PIC assembly, and transcriptional activation. (A) In WT cells, the UAS-bound Gcn4 recruits the SAGA complex (two-headed arrow) to the *ARG1* promoter, upon which SAGA acetylates (Ac) nucleosomes and delivers TBP to the core promoter, leading to PIC assembly and transcriptional activation. In *taf9* mutant cells, although Gcn4 interaction with SAGA is intact, SAGA occupancy was reduced at the $ARG1_{UAS}$. Consistent with the reduced SAGA levels, TBP and H3 K9/14Ac levels were also diminished by the *taf9* mutation. However, PIC (TFIIB and RNAP II) assembly was not reduced. Robust recruitment of the mediator (Gal11) was seen in WT and *taf9* mutant cells, leading to efficient PIC assembly at the $ARG1_{core}$ promoter. (B) The Taf9 CRD is required for TFIID occupancy (single arrow) at the *TRP3* core promoter. *TRP3* is a Gcn4-induced target gene that is SAGA depleted but TFIID dominated. TFIID occupancy and PIC assembly are critically dependent on the Taf9 CRD. (C) Dual recruitment of SAGA and TFIID at *BNA1* and *MET28* promoters is dependent on the Taf9 CRD. *BNA1* and *MET28* are Gcn4-induced genes that are bound by both TFIID and SAGA. The *taf9-tCRD2* mutation impairs SAGA and TFIID occupancy, as well as PIC assembly, at the *BNA1* and *MET28* promoters.

pendent genes are also Taf9 CRD dependent for activation in SM (Fig. 3A), indicating that the Taf9 CRD is required for transcriptional activity of SAGA *in vivo*. Consistent with these results, ChIP analysis showed that SAGA occupancy was severely reduced (Fig. 6C and E) in the *taf9* CRD mutant. Moreover, the histone H3 K9/14Ac carried out by SAGA was reduced by about 50% in the *ARG1* gene UAS and core promoter regions (Fig. 6D), indicating that SAGA acetylation function is also compromised *in vivo* by the *taf9-tCRD2* mutation.

The Taf9 CRD is a common determinant of SAGA and TFIID promoter occupancy. SAGA and TFIID have distinct promoter specificities, and accordingly, yeast promoters have been classified

as TFIID or SAGA dominated (18, 19), including in recent genomic studies (15, 68). SAGA recruitment to the UAS is through direct activator interactions (51, 63, 69, 70). TFIID recruitment to promoters is mediated via Rap1 (2, 60), as well as through core promoter interactions (19). There are also examples of promoters under dual regulation by SAGA and TFIID. The *RNR3* gene promoter has been shown to bind TFIID and requires the acetylation and TBP recruitment functions of SAGA (71). SAGA and TFIID are also recruited to promoters in response to heat shock and DNA damage (17, 72). Thus, the SAGA and TFIID occupancies are dependent on the promoter context and are also activator dependent.

We examined the requirement for the Taf9 CRD for TFIID and SAGA occupancy at Gcn4-induced gene promoters. Our studies identified distinct promoter classes: those that are bound by SAGA (Spt7) but not TFIID (Taf11), such as *ARG1*; those that are bound by TFIID but not SAGA, such as *TRP3*; and those that are bound by both SAGA and TFIID, such as *MET28* and *BNA1* (Fig. 9). Notably, the SAGA and/or TFIID occupancies in the UAS and core promoter regions, respectively, of these gene promoters were highly dependent on the Taf9 CRD. Thus, Gcn4 appears to stimulate transcription in a promoter-dependent manner by differentially engaging the TFIID and SAGA coactivator modules (Fig. 9).

Although the Taf9 CRD is required for PIC assembly at most promoters examined, *ARG1* was an exception (Fig. 9). Several studies have demonstrated TBP recruitment function for SAGA (reviewed in reference 2). In the results presented here, SAGA recruitment at $ARG1_{UAS}$ was lost in the *taf9* CRD mutant (Fig. 6), and a consequent reduction in TBP recruitment at the $ARG1_{core}$ promoter was observed (Fig. 8). Moreover, previous studies showed that SAGA and the mediator are independently recruited to $ARG1_{UAS}$ by Gcn4 (7), and consistent with this, the mediator was efficiently recruited to $ARG1_{UAS}$ in the *taf9* mutant (Fig. 8A and 9). Thus, it appears that the robust levels of the mediator and the residual level of TBP could result in unimpaired PIC levels at the $ARG1_{core}$ promoter.

As discussed above, we have shown a requirement for the Taf9 CRD for SAGA occupancy of the UAS and TFIID occupancy of core promoter regions of multiple genes (Fig. 6). We demonstrated that Gcn4 recruitment to the Taf9 CRD-dependent genes under SM was comparable in the WT and the *taf9* mutant, indicating that the transcriptional activation defect is not a consequence of impaired activator binding to the UAS. Moreover, the interaction of Gcn4 with SAGA in cell extracts was not impaired by the Taf9 CRD mutation. Tra1 and Taf12, two SAGA subunits previously shown to interact with the Gcn4 activation domain (51, 63, 69), are efficiently coimmunoprecipitated in a complex with Spt7 (Fig. 5D), and the same subunits were also pulled down by Gcn4 (Fig. 5E); therefore, it is likely that the CRD is dispensable for Gcn4 interaction with SAGA *in vivo*.

How might the Taf9 CRD function in SAGA and TFIID promoter occupancy? One possibility is that truncation of the Taf9 CRD impairs interaction with a component of SAGA and TFIID. In this context, we hypothesized two potential candidates: Taf6, as the heterodimerization partner, and Taf5, recently shown to promote Taf6-Taf9 interaction through the Taf6 C-terminal HEAT domain (73). Accordingly, we overexpressed *TAF6* and *TAF5* in the *taf9-tCRD2* mutant strain and found that neither could suppress the mutant phenotype (data not shown). It remains to be seen what factors, if any, have genetic and/or physical interactions with the Taf9 CRD.

Previous reports showed that the Taf9 CRD interacts with downstream promoter element (DPE)-containing promoters in *Drosophila* (32), which was shown to be required for sequence-specific DNA binding to the DPE as a heterodimer in association with Taf6. Furthermore, the human Taf9 C-terminal conserved region was shown to have both intrinsic sequence-independent DNA binding activity and sequence-dependent DNA binding to the DPEs of core promoters (25, 33). Although no DPEs have been found in yeast so far (references 2 and 32 and our unpublished data), it is possible that the Taf9 CRD, in association with Taf6, provides a sequence-independent DNA binding activity at core promoters of the Taf9 CRD-dependent genes in yeast. Alternatively, it is possible that interaction of TFIID and SAGA with chromatin is dependent on the Taf9 CRD. In this scenario, TFIID has been shown to interact with chromatin through specific TAF subunits in a manner that recognizes specific histone modifications, such as Taf3 interaction with H3K4Me3 histones (74–76) or the Taf1/Bdf1 interaction with acetylated histone H4 (77). Also, the mammalian TFIID subunits Taf1, Taf4, Taf6, and Taf12 also appear to interact with DNA (25), thereby providing additional interactions with promoter DNA. SAGA, too, contains multiple chromatin interaction motifs (24), and thus, the Taf9 CRD could promote SAGA interaction with chromatin. Even though the H3 K9/14Ac was reduced by only ~50% in the *taf9* mutant, we cannot rule out the possibility of inefficient SAGA binding to poorly acetylated chromatin. The interplay between these chromatin-interacting domains and the Taf9 CRD alone, or in conjunction with Taf6, could stabilize TFIID and SAGA on chromatin in promoters *in vivo*. Thus, in the absence of the Taf9 CRD, it seems possible that TFIID and SAGA have high off rates from chromatin, thereby leading to diminished occupancy.

In summary, we have demonstrated that the Taf9 CRD is essential for TFIID and SAGA occupancy at gene promoters to support transcriptional activation by Gcn4. Our results also show that Gcn4 employs a common strategy, using the Taf9 CRD to potentiate TBP delivery and PIC assembly during transcriptional activation. Altogether, this study highlights the importance of a conserved domain in shared TAFs, other than the histone fold domain, as a common determinant of SAGA and TFIID promoter occupancy and transcriptional activation. Future studies on other conserved domains in shared TAF subunits could uncover the full range of domain requirements and their specialization, if any, in the two transcriptional regulatory complexes.

ACKNOWLEDGMENTS

We thank Alan Hinnebusch (National Institutes of Health), Jerry Workman (Stowers Institute of Medical Research), Tetsuro Kokubo (Yokohama City University, Japan), Tony Weil (Vanderbilt University), Steven Buratowski (Harvard Medical School), and Shelley Berger (University of Pennsylvania) for providing antibodies and strains; Jayasha Shandilya for carrying out the initial genetic screen; Jerry Workman, Alan Hinnebusch, and Swami Venkatesh for discussions and comments on the manuscript; Genotypic Technologies, Bangalore, India, for microarray hybridizations; and Jeffrey Townsend (Yale University) and Rashi Gupta for advice on BAGEL analysis.

M.S., I.S., R.P.S., and R.D. were supported by Junior and Senior Research Fellowships from CSIR; S.S. was supported by a Senior Research Fellowship from ICMR. R.S. acknowledges support from the PRISM project at IMSc, funded by DAE, Government of India. This work was funded

by a research grant from CSIR, by partial support under DST-PURSE, by UPOE, and by UGC-RNW grants to K.N.

R.D. performed all experiments during revision of the manuscript.

REFERENCES

1. **Lee TI, Rinaldi NJ, Robert F, Odom DT, Bar-Joseph Z, Gerber GK, Hannett NM, Harbison CT, Thompson CM, Simon I, Zeitlinger J, Jennings EG, Murray HL, Gordon DB, Ren B, Wyrick JJ, Tagne JB, Volkert TL, Fraenkel E, Gifford DK, Young RA.** 2002. Transcriptional regulatory networks in *Saccharomyces cerevisiae*. Science **298:**799–804. http://dx.doi.org/10.1126/science.1075090.
2. **Hahn S, Young ET.** 2011. Transcriptional regulation in Saccharomyces cerevisiae: transcription factor regulation and function, mechanisms of initiation, and roles of activators and coactivators. Genetics **189:**705–736. http://dx.doi.org/10.1534/genetics.111.127019.
3. **Venters BJ, Pugh BF.** 2009. How eukaryotic genes are transcribed. Crit. Rev. Biochem. Mol. Biol. **44:**117–141.
4. **Lee KK, Workman JL.** 2007. Histone acetyltransferase complexes: one size doesn't fit all. Nat. Rev. Mol. Cell Biol. **8:**284–295. http://dx.doi.org/10.1038/nrm2145.
5. **Thomas MC, Chiang CM.** 2006. The general transcription machinery and general cofactors. Crit. Rev. Biochem. Mol. Biol. **41:**105–178. http://dx.doi.org/10.1080/10409230600648736.
6. **Hinnebusch AG, Natarajan K.** 2002. Gcn4p, a master regulator of gene expression, is controlled at multiple levels by diverse signals of starvation and stress. Eukaryot. Cell **1:**22–32. http://dx.doi.org/10.1128/EC.01.1.22-32.2002.
7. **Qiu H, Hu C, Zhang F, Hwang GJ, Swanson MJ, Boonchird C, Hinnebusch AG.** 2005. Interdependent recruitment of SAGA and Srb mediator by transcriptional activator Gcn4p. Mol. Cell. Biol. **25:**3461–3474. http://dx.doi.org/10.1128/MCB.25.9.3461-3474.2005.
8. **Govind CK, Yoon S, Qiu H, Govind S, Hinnebusch AG.** 2005. Simultaneous recruitment of coactivators by Gcn4p stimulates multiple steps of transcription in vivo. Mol. Cell. Biol. **25:**5626–5638. http://dx.doi.org/10.1128/MCB.25.13.5626-5638.2005.
9. **Natarajan K, Jackson BM, Zhou H, Winston F, Hinnebusch AG.** 1999. Transcriptional activation by Gcn4p involves independent interactions with SWI/SNF complex and SRB/mediator. Mol. Cell **4:**657–664. http://dx.doi.org/10.1016/S1097-2765(00)80217-8.
10. **Zhang F, Sumibcay L, Hinnebusch AG, Swanson MJ.** 2004. A triad of subunits from the Gal11/tail domain of Srb mediator is an in vivo target of transcriptional activator Gcn4p. Mol. Cell. Biol. **24:**6871–6886. http://dx.doi.org/10.1128/MCB.24.15.6871-6886.2004.
11. **Jedidi I, Zhang F, Qiu H, Stahl SJ, Palmer I, Kaufman JD, Nadaud PS, Mukherjee S, Wingfield PT, Jaroniec CP, Hinnebusch AG.** 2010. Activator Gcn4 employs multiple segments of Med15/Gal11, including the KIX domain, to recruit mediator to target genes in vivo. J. Biol. Chem. **285:**2438–2455. http://dx.doi.org/10.1074/jbc.M109.071589.
12. **Cheung AC, Cramer P.** 2012. A movie of RNA polymerase II transcription. Cell **149:**1431–1437. http://dx.doi.org/10.1016/j.cell.2012.06.006.
13. **Klein C, Struhl K.** 1994. Increased recruitment of TATA-binding protein to the promoter by transcriptional activation domains in vivo. Science **266:**280–282. http://dx.doi.org/10.1126/science.7939664.
14. **Kuras L, Struhl K.** 1999. Binding of TBP to promoters *in vivo* is stimulated by activators and requires Pol II holoenzyme. Nature **399:**609–613. http://dx.doi.org/10.1038/21239.
15. **Huisinga KL, Pugh BF.** 2004. A genome-wide housekeeping role for TFIID and a highly regulated stress-related role for SAGA in *Saccharomyces cerevisiae*. Mol. Cell **13:**573–585. http://dx.doi.org/10.1016/S1097-2765(04)00087-5.
16. **Rhee HS, Pugh BF.** 2012. Genome-wide structure and organization of eukaryotic pre-initiation complexes. Nature **483:**295–301. http://dx.doi.org/10.1038/nature10799.
17. **Zanton SJ, Pugh BF.** 2006. Full and partial genome-wide assembly and disassembly of the yeast transcription machinery in response to heat shock. Genes Dev. **20:**2250–2265. http://dx.doi.org/10.1101/gad.1437506.
18. **Kuras L, Kosa P, Mencia M, Struhl K.** 2000. TAF-containing and TAF-independent forms of transcriptionally active TBP in vivo. Science **288:**1244–1248. http://dx.doi.org/10.1126/science.288.5469.1244.
19. **Li XY, Bhaumik SR, Green MR.** 2000. Distinct classes of yeast promoters revealed by differential TAF recruitment. Science **288:**1242–1244. http://dx.doi.org/10.1126/science.288.5469.1242.
20. **Lee TI, Causton HC, Holstege FC, Shen WC, Hannett N, Jennings EG, Winston F, Green MR, Young RA.** 2000. Redundant roles for the TFIID and SAGA complexes in global transcription. Nature **405:**701–704. http://dx.doi.org/10.1038/35015104.
21. **Grant PA, Schieltz D, Pray-Grant MG, Steger DJ, Reese JC, Yates JR, III, Workman JL.** 1998. A subset of TAF(II)s are integral components of the SAGA complex required for nucleosome acetylation and transcriptional stimulation. Cell **94:**45–53. http://dx.doi.org/10.1016/S0092-8674(00)81220-9.
22. **Wieczorek E, Brand M, Jacq X, Tora L.** 1998. Function of TAF_{II}-containing complex without TBP in transcription by RNA polymerase II. Nature **393:**187–191. http://dx.doi.org/10.1038/30283.
23. **Drysdale CM, Jackson BM, McVeigh R, Klebanow ER, Bai Y, Kokubo T, Swanson M, Nakatani Y, Weil PA, Hinnebusch AG.** 1998. The Gcn4p activation domain interacts specifically in vitro with RNA polymerase II holoenzyme, TFIID, and the Adap-Gcn5p coactivator complex. Mol. Cell. Biol. **18:**1711–1724.
24. **Spedale G, Timmers HT, Pijnappel WW.** 2012. ATAC-king the complexity of SAGA during evolution. Genes Dev. **26:**527–541. http://dx.doi.org/10.1101/gad.184705.111.
25. **Shao H, Revach M, Moshonov S, Tzuman Y, Gazit K, Albeck S, Unger T, Dikstein R.** 2005. Core promoter binding by histone-like TAF complexes. Mol. Cell. Biol. **25:**206–219. http://dx.doi.org/10.1128/MCB.25.1.206-219.2005.
26. **Chen Z, Manley JL.** 2003. In vivo functional analysis of the histone 3-like TAF9 and a TAF9-related factor, TAF9L. J. Biol. Chem. **278:**35172–35183. http://dx.doi.org/10.1074/jbc.M304241200.
27. **Moqtaderi Z, Keaveney M, Struhl K.** 1998. The histone H3-like TAF is broadly required for transcription in yeast. Mol. Cell **2:**675–682. http://dx.doi.org/10.1016/S1097-2765(00)80165-3.
28. **Michel B, Komarnitsky P, Buratowski S.** 1998. Histone-like TAFs are essential for transcription in vivo. Mol. Cell **2:**663–673. http://dx.doi.org/10.1016/S1097-2765(00)80164-1.
29. **Shen WC, Bhaumik SR, Causton HC, Simon I, Zhu X, Jennings EG, Wang TH, Young RA, Green MR.** 2003. Systematic analysis of essential yeast TAFs in genome-wide transcription and preinitiation complex assembly. EMBO J. **22:**3395–3402. http://dx.doi.org/10.1093/emboj/cdg336.
30. **Xie X, Kokubo T, Cohen SL, Mirza UA, Hoffmann A, Chait BT, Roeder RG, Nakatani Y, Burley SK.** 1996. Structural similarity between TAFs and the heterotetrameric core of the histone octamer. Nature **380:**316–322. http://dx.doi.org/10.1038/380316a0.
31. **Sanders SL, Jennings J, Canutescu A, Link AJ, Weil PA.** 2002. Proteomics of the eukaryotic transcription machinery: identification of proteins associated with components of yeast TFIID by multidimensional mass spectrometry. Mol. Cell. Biol. **22:**4723–4738. http://dx.doi.org/10.1128/MCB.22.13.4723-4738.2002.
32. **Burke TW, Kadonaga JT.** 1997. The downstream core promoter element, DPE, is conserved from *Drosophila* to humans and is recognized by $TAF_{II}60$ of *Drosophila*. Genes Dev. **11:**3020–3031. http://dx.doi.org/10.1101/gad.11.22.3020.
33. **Sengupta T, Cohet N, Morle F, Bieker JJ.** 2009. Distinct modes of gene regulation by a cell-specific transcriptional activator. Proc. Natl. Acad. Sci. U. S. A. **106:**4213–4218. http://dx.doi.org/10.1073/pnas.0808347106.
34. **Macpherson N, Measday V, Moore L, Andrews B.** 2000. A yeast taf17 mutant requires the Swi6 transcriptional activator for viability and shows defects in cell cycle-regulated transcription. Genetics **154:**1561–1576.
35. **Ausubel FM, Brent R, Kingston RE, Moore DD, Seidman JG, Smith JA, Struhl K.** 2002. Short protocols in molecular biology, 5th ed, vol 1. John Wiley & Sons, Inc., Hoboken, NJ.
36. **Gietz RD, Woods RA.** 2002. Transformation of yeast by lithium acetate/single-stranded carrier DNA/polyethylene glycol method. Methods Enzymol. **350:**87–96. http://dx.doi.org/10.1016/S0076-6879(02)50957-5.
37. **Kohrer K, Domdey H.** 1991. Preparation of high molecular weight RNA. Methods Enzymol. **194:**398–405. http://dx.doi.org/10.1016/0076-6879(91)94030-G.
38. **Livak KJ, Schmittgen TD.** 2001. Analysis of relative gene expression data using real-time quantitative PCR and the $2^{-\Delta\Delta CT}$ method. Methods **25:**402–408. http://dx.doi.org/10.1006/meth.2001.1262.
39. **Pfaffl MW.** 2001. A new mathematical model for relative quantification in

real-time RT-PCR. Nucleic Acids Res. **29:**e45. http://dx.doi.org/10.1093/nar/29.9.e45.
40. **Tusher VG, Tibshirani R, Chu G.** 2001. Significance analysis of microarrays applied to the ionizing radiation response. Proc. Natl. Acad. Sci. U. S. A. **98:**5116–5121. http://dx.doi.org/10.1073/pnas.091062498.
41. **Townsend JP, Hartl DL.** 2002. Bayesian analysis of gene expression levels: statistical quantification of relative mRNA level across multiple strains or treatments. Genome Biol. **3:**RESEARCH0071.
42. **Natarajan K, Meyer MR, Jackson BM, Slade D, Roberts CJ, Hinnebusch AG, Marton MJ.** 2001. Transcriptional profiling shows that Gcn4p is a master regulator of gene expression during amino acid starvation in yeast. Mol. Cell. Biol. **21:**4347–4368. http://dx.doi.org/10.1128/MCB.21.13.4347-4368.2001.
43. **Woontner M, Wade PA, Bonner J, Jaehning JA.** 1991. Transcriptional activation in an improved whole-cell extract from *Saccharomyces cerevisiae*. Mol. Cell. Biol. **11:**4555–4560.
44. **Qiu H, Hu C, Yoon S, Natarajan K, Swanson MJ, Hinnebusch AG.** 2004. An array of coactivators is required for optimal recruitment of TATA binding protein and RNA polymerase II by promoter-bound Gcn4p. Mol. Cell. Biol. **24:**4104–4117. http://dx.doi.org/10.1128/MCB.24.10.4104-4117.2004.
45. **Govind CK, Zhang F, Qiu H, Hofmeyer K, Hinnebusch AG.** 2007. Gcn5 promotes acetylation, eviction, and methylation of nucleosomes in transcribed coding regions. Mol. Cell **25:**31–42. http://dx.doi.org/10.1016/j.molcel.2006.11.020.
46. **Swanson MJ, Qiu H, Sumibcay L, Krueger A, Kim SJ, Natarajan K, Yoon S, Hinnebusch AG.** 2003. A multiplicity of coactivators is required by Gcn4p at individual promoters in vivo. Mol. Cell. Biol. **23:**2800–2820. http://dx.doi.org/10.1128/MCB.23.8.2800-2820.2003.
47. **Cigan AM, Bushman JL, Boal TR, Hinnebusch AG.** 1993. A protein complex of translational regulators of *GCN4* is the guanine nucleotide exchange factor for eIF-2 in yeast. Proc. Natl. Acad. Sci. U. S. A. **90:**5350–5354. http://dx.doi.org/10.1073/pnas.90.11.5350.
48. **Natarajan K, Jackson BM, Rhee E, Hinnebusch AG.** 1998. yTAF$_{II}$61 has a general role in RNA polymerase II transcription and is required by Gcn4p to recruit the SAGA coactivator complex. Mol. Cell **2:**683–692. http://dx.doi.org/10.1016/S1097-2765(00)80166-5.
49. **Candau R, Berger SL.** 1996. Structural and functional analysis of yeast putative adaptors. J. Biol. Chem. **271:**5237–5245. http://dx.doi.org/10.1074/jbc.271.9.5237.
50. **Takahata S, Kasahara K, Kawaichi M, Kokubo T.** 2004. Autonomous function of the amino-terminal inhibitory domain of TAF1 in transcriptional regulation. Mol. Cell. Biol. **24:**3089–3099. http://dx.doi.org/10.1128/MCB.24.8.3089-3099.2004.
51. **Brown CE, Howe L, Sousa K, Alley SC, Carrozza MJ, Tan S, Workman JL.** 2001. Recruitment of HAT complexes by direct activator interactions with the ATM-related Tra1 subunit. Science **292:**2333–2337. http://dx.doi.org/10.1126/science.1060214.
52. **Kokubo T, Yamashita S, Horikoshi M, Roeder RG, Nakatani Y.** 1994. Interaction between the N-terminal domain of the 230-kDa subunit and the TATA box-binding subunit of TFIID negatively regulates TATA-box binding. Proc. Natl. Acad. Sci. U. S. A. **91:**3520–3524. http://dx.doi.org/10.1073/pnas.91.9.3520.
53. **Klebanow ER, Poon D, Zhou S, Weil PA.** 1996. Isolation and characterization of *TAF25*, an essential yeast gene that encodes an RNA polymerase II-specific TATA-binding protein-associated factor. J. Biol. Chem. **271:**13706–13715. http://dx.doi.org/10.1074/jbc.271.23.13706.
54. **Hinnebusch AG.** 1992. General and pathway-specific regulatory mechanisms controlling the synthesis of amino acid biosynthetic enzymes in *Saccharomyces cerevisiae*, p 319–414. *In* Broach JR, Jones EW, Pringle JR (ed), The molecular and cellular biology of the yeast *Saccharomyces*: gene expression. Cold Spring Harbor Laboratory Press, Cold Spring Harbor, NY.
55. **Milgrom E, West RW, Jr, Gao C, Shen WC.** 2005. TFIID and Spt-Ada-Gcn5-acetyltransferase functions probed by genome-wide synthetic genetic array analysis using a *Saccharomyces cerevisiae taf9-ts* allele. Genetics **171:**959–973. http://dx.doi.org/10.1534/genetics.105.046557.
56. **Rodriguez-Navarro S.** 2009. Insights into SAGA function during gene expression. EMBO Rep. **10:**843–850. http://dx.doi.org/10.1038/embor.2009.168.
57. **Wyce A, Xiao T, Whelan KA, Kosman C, Walter W, Eick D, Hughes TR, Krogan NJ, Strahl BD, Berger SL.** 2007. H2B ubiquitylation acts as a barrier to Ctk1 nucleosomal recruitment prior to removal by Ubp8 within a SAGA-related complex. Mol. Cell **27:**275–288. http://dx.doi.org/10.1016/j.molcel.2007.01.035.
58. **Desmoucelles C, Pinson B, Saint-Marc C, Daignan-Fornier B.** 2002. Screening the yeast "disruptome" for mutants affecting resistance to the immunosuppressive drug, mycophenolic acid. J. Biol. Chem. **277:**27036–27044. http://dx.doi.org/10.1074/jbc.M111433200.
59. **Hinnebusch AG, Lucchini G, Fink GR.** 1985. A synthetic *HIS4* regulatory element confers general amino acid control on the cytochrome *c* gene *CYC1* of yeast. Proc. Natl. Acad. Sci. U. S. A. **82:**498–502. http://dx.doi.org/10.1073/pnas.82.2.498.
60. **Garbett KA, Tripathi MK, Cencki B, Layer JH, Weil PA.** 2007. Yeast TFIID serves as a coactivator for Rap1p by direct protein-protein interaction. Mol. Cell. Biol. **27:**297–311. http://dx.doi.org/10.1128/MCB.01558-06.
61. **Mencia M, Moqtaderi Z, Geisberg JV, Kuras L, Struhl K.** 2002. Activator-specific recruitment of TFIID and regulation of ribosomal protein genes in yeast. Mol. Cell **9:**823–833. http://dx.doi.org/10.1016/S1097-2765(02)00490-2.
62. **Harbison CT, Gordon DB, Lee TI, Rinaldi NJ, Macisaac KD, Danford TW, Hannett NM, Tagne JB, Reynolds DB, Yoo J, Jennings EG, Zeitlinger J, Pokholok DK, Kellis M, Rolfe PA, Takusagawa KT, Lander ES, Gifford DK, Fraenkel E, Young RA.** 2004. Transcriptional regulatory code of a eukaryotic genome. Nature **431:**99–104. http://dx.doi.org/10.1038/nature02800.
63. **Knutson BA, Hahn S.** 2011. Domains of Tra1 important for activator recruitment and transcription coactivator functions of SAGA and NuA4 complexes. Mol. Cell. Biol. **31:**818–831. http://dx.doi.org/10.1128/MCB.00687-10.
64. **Bhaumik SR, Green MR.** 2001. SAGA is an essential in vivo target of the yeast acidic activator Gal4p. Genes Dev. **15:**1935–1945. http://dx.doi.org/10.1101/gad.911401.
65. **Ohtsuki K, Kasahara K, Shirahige K, Kokubo T.** 2010. Genome-wide localization analysis of a complete set of Tafs reveals a specific effect of the taf1 mutation on Taf2 occupancy and provides indirect evidence for different TFIID conformations at different promoters. Nucleic Acids Res. **38:**1805–1820. http://dx.doi.org/10.1093/nar/gkp1172.
66. **Buratowski S.** 2009. Progression through the RNA polymerase II CTD cycle. Mol. Cell **36:**541–546. http://dx.doi.org/10.1016/j.molcel.2009.10.019.
67. **Venters BJ, Wachi S, Mavrich TN, Andersen BE, Jena P, Sinnamon AJ, Jain P, Rolleri NS, Jiang C, Hemeryck-Walsh C, Pugh BF.** 2011. A comprehensive genomic binding map of gene and chromatin regulatory proteins in Saccharomyces. Mol. Cell **41:**480–492. http://dx.doi.org/10.1016/j.molcel.2011.01.015.
68. **Zanton SJ, Pugh BF.** 2004. Changes in genomewide occupancy of core transcriptional regulators during heat stress. Proc. Natl. Acad. Sci. U. S. A. **101:**16843–16848. http://dx.doi.org/10.1073/pnas.0404988101.
69. **Brzovic PS, Heikaus CC, Kisselev L, Vernon R, Herbig E, Pacheco D, Warfield L, Littlefield P, Baker D, Klevit RE, Hahn S.** 2011. The acidic transcription activator Gcn4 binds the mediator subunit Gal11/Med15 using a simple protein interface forming a fuzzy complex. Mol. Cell **44:**942–953. http://dx.doi.org/10.1016/j.molcel.2011.11.008.
70. **Klein J, Nolden M, Sanders SL, Kirchner J, Weil PA, Melcher K.** 2003. Use of a genetically introduced cross-linker to identify interaction sites of acidic activators within native transcription factor IID and SAGA. J. Biol. Chem. **278:**6779–6786. http://dx.doi.org/10.1074/jbc.M212514200.
71. **Zhang H, Kruk JA, Reese JC.** 2008. Dissection of coactivator requirement at RNR3 reveals unexpected contributions from TFIID and SAGA. J. Biol. Chem. **283:**27360–27368. http://dx.doi.org/10.1074/jbc.M803831200.
72. **Ghosh S, Pugh BF.** 2011. Sequential recruitment of SAGA and TFIID in a genomic response to DNA damage in Saccharomyces cerevisiae. Mol. Cell. Biol. **31:**190–202. http://dx.doi.org/10.1128/MCB.00317-10.
73. **Scheer E, Delbac F, Tora L, Moras D, Romier C.** 2012. TFIID TAF6/TAF9 complex formation involves the HEAT repeat-containing C-terminal domain of TAF6 and is modulated by TAF5. J. Biol. Chem. **287:**27580–27592. http://dx.doi.org/10.1074/jbc.M112.379206.
74. **Lauberth SM, Nakayama T, Wu X, Ferris AL, Tang Z, Hughes SH, Roeder RG.** 2013. H3K4me3 interactions with TAF3 regulate preinitiation complex assembly and selective gene activation. Cell **152:**1021–1036. http://dx.doi.org/10.1016/j.cell.2013.01.052.
75. **van Ingen H, van Schaik FM, Wienk H, Ballering J, Rehmann H,**

Dechesne AC, Kruijzer JA, Liskamp RM, Timmers HT, Boelens R. 2008. Structural insight into the recognition of the H3K4me3 mark by the TFIID subunit TAF3. Structure **16:**1245–1256. http://dx.doi.org/10.1016/j.str.2008.04.015.

76. **Vermeulen M, Mulder KW, Denissov S, Pijnappel WW, van Schaik FM, Varier RA, Baltissen MP, Stunnenberg HG, Mann M, Timmers HT.** 2007. Selective anchoring of TFIID to nucleosomes by trimethylation of histone H3 lysine 4. Cell **131:**58–69. http://dx.doi.org/10.1016/j.cell.2007.08.016.
77. **Jacobson RH, Ladurner AG, King DS, Tjian R.** 2000 Structure and function of a human TAFII250 double bromodomain module. Science **288:**1422–1425. http://dx.doi.org/10.1126/science.288.5470.1422.